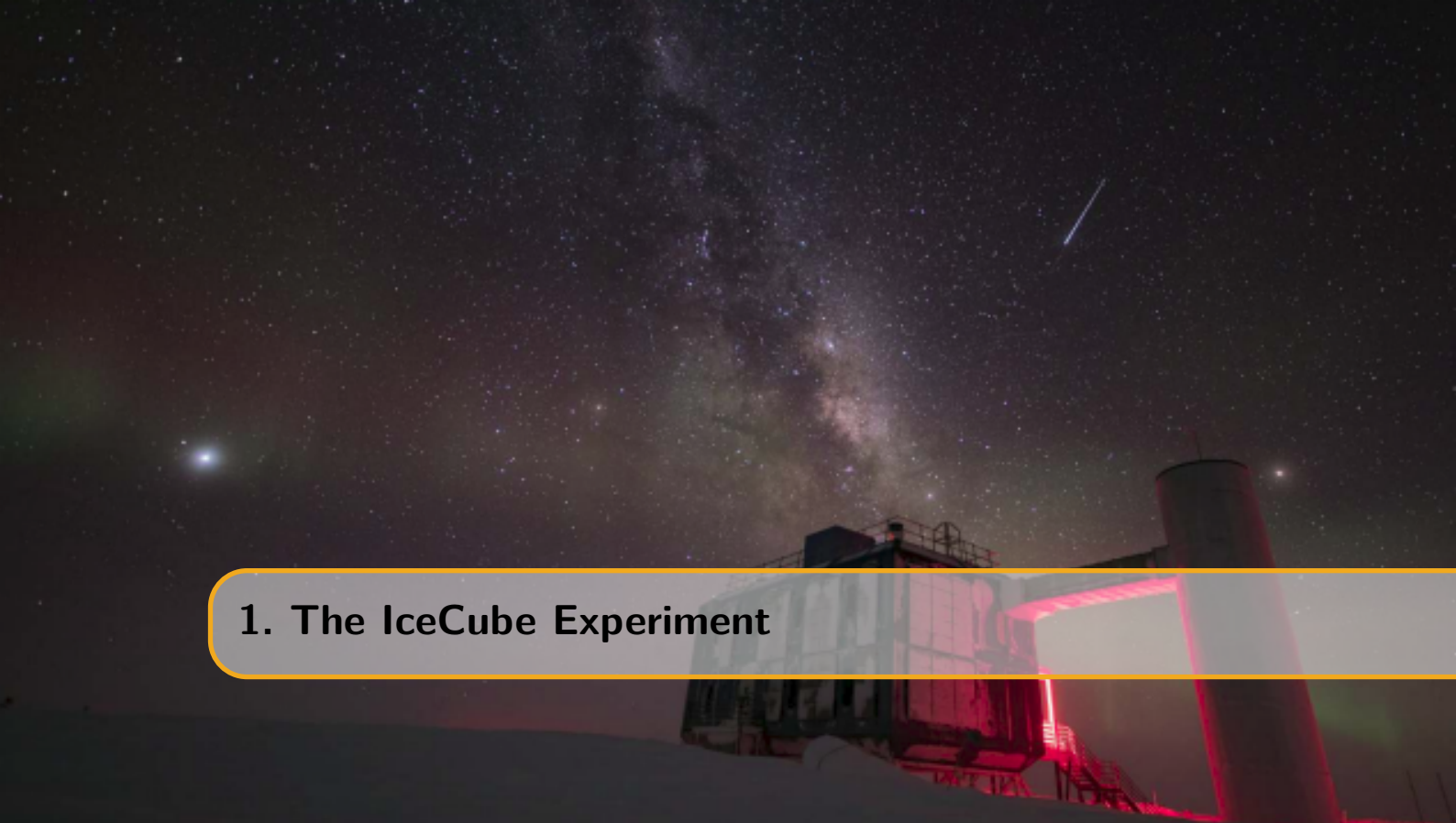


Table of Contents

| | | |
|------------|---|-----------|
| 1 | The IceCube Experiment | 3 |
| 1.1 | Geometry | 3 |
| 1.1.1 | In-ice array | 5 |
| 1.1.2 | DeepCore | 5 |
| 1.1.3 | IceTop | 5 |
| 1.1.4 | IceCube coordinate system | 6 |
| 1.2 | Hardware components | 7 |
| 1.2.1 | Digital optical modules | 7 |
| 1.2.2 | Calibration | 9 |
| 1.2.3 | Cable systems | 9 |
| 1.2.4 | IceCube laboratory | 9 |
| 1.3 | Deployment | 11 |
| 1.4 | Data taking | 11 |
| 1.4.1 | Triggers | 11 |
| 1.4.2 | Filters | 13 |
| 1.4.3 | Data handling | 14 |
| 1.5 | Antarctic ice | 14 |
| 1.5.1 | Ice simulation | 14 |
| 1.5.2 | Systematic uncertainties | 15 |
| 1.6 | IceCube event topology | 16 |
| 1.7 | Future upgrades | 16 |
| 1.7.1 | IceCube Upgrade | 17 |
| 1.7.2 | IceCube Gen2 | 17 |
| 1.8 | Beyond the Standard Model searches | 19 |
| 1.8.1 | Lorentz invariance violation | 20 |
| 1.8.2 | Dark matter | 20 |
| 1.8.3 | Magnetic monopoles | 21 |
| 1.9 | Discussion | 22 |
| | Bibliography | 23 |



1. The IceCube Experiment

Computers are useless; they can only give you answers ~ Pablo Picasso

IceCube is a neutrino observatory located near the Amundsen-Scott South Pole Station close to the geographic South Pole. Experiments that search for astrophysical neutrinos need to be constructed with enormous instrumented volumes. IceCube is the first gigaton neutrino detector ever built and was designed specifically for this case. It is buried beneath the surface of the Antarctic ice, starting from around 1450 meters of depth and extending to around 2500 meters (~ 300 meters above bedrock). The ice acts as a medium for both the interaction of a neutrino and light propagation. This chapter serves as a general overview of the several components of IceCube detector together with an introduction to the data processing.

The main goal of the IceCube experiment is to learn more about the distant sources that we believe to be responsible for the production of the highest-energy cosmic rays. As indicated in Section ??, neutrinos are crucial in gaining information about these far away sources. Large-scale detectors are necessary to observe the faint flux of neutrinos with very high energies. Detecting the Cherenkov radiation (Chapter ??) from neutrino interactions is the best way to observe these weakly interacting particles. Because hadronic, electromagnetic and muonic components from these interactions require a medium that extends to a couple of kilometers and has good light propagation characteristics, the South Pole ice sheet acts as a near ideal component of the detector. As a proof of concept, the AMANDA (Antarctic Muon And Neutrino Detector Array) experiment was built between 1996 and 2000 to show that neutrinos with energies above 50 GeV could be detected in the Antarctic ice [147, 148]. After construction was finalized, this detector consisted of 677 optical modules mounted on 19 separate strings that are spread out in a rough circle with a diameter of around 200 meters. The strings were deployed by first “drilling” holes in the ice with a hot-water hose, showing that this specific drilling technique works and can be used on larger scales. After some years of data taking, it was clear that high-energy neutrinos could be observed, paving the way for the much larger IceCube project [149].

1.1 Geometry

The IceCube detector consists of three main parts that act as different purpose physics detectors. The *in-ice* *IceCube* detector is the main component and consists of 4680 digital optical modules.

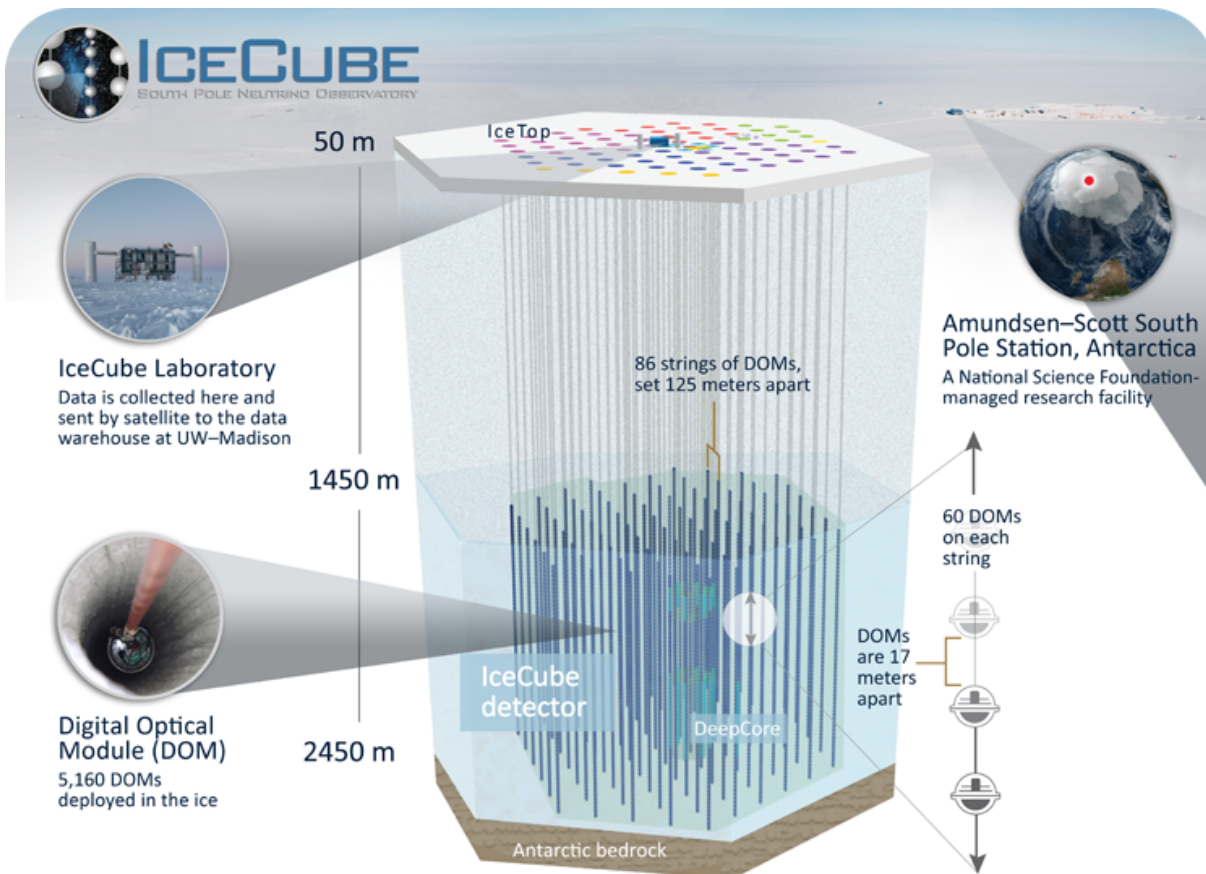


Figure 1.1: Illustration of the IceCube South Pole neutrino observatory.

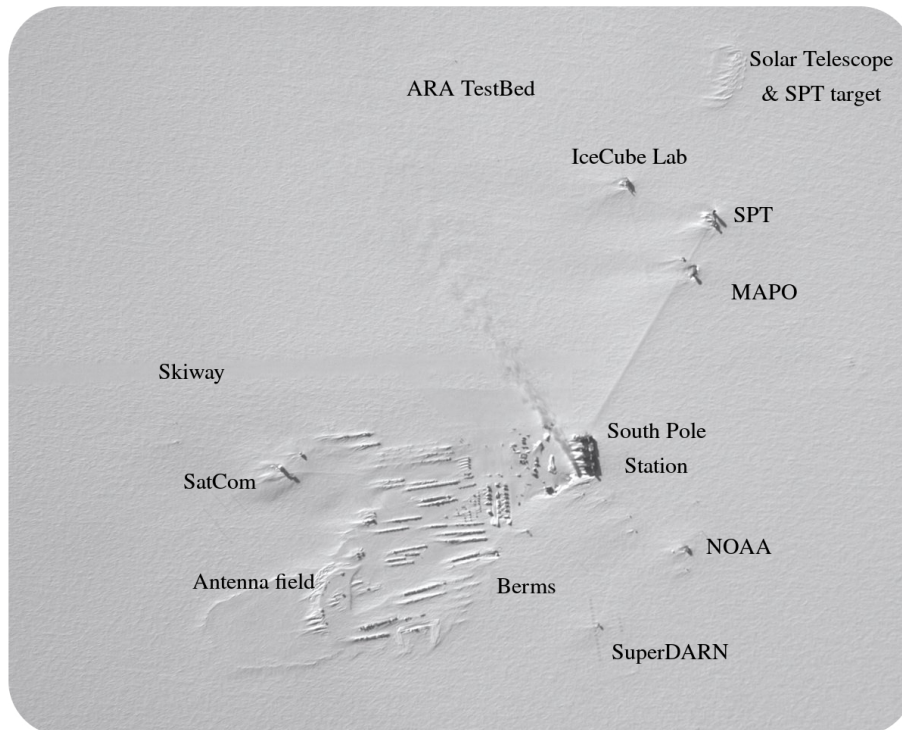


Figure 1.2: Aerial view of the South Pole. The main buildings and experimental setups are indicated in the figure. The exhaust of the South Pole Station is also visible.

In its core, a denser subdetector, *DeepCore*, significantly enhances the capabilities for low-energy events of the observatory in a limited volume. The center of the DeepCore array consists of 480 sensors. On the surface of the ice, water tanks with optical modules inside are spread out over an area of approximately 1 km^2 and make up the *IceTop detector*. This surface array was built as a cosmic ray detector and veto for the in-ice array. The three components combined make the facility a multipurpose physics detector. Figure 1.1 shows the layout of the detector.

1.1.1 In-ice array

The in-ice array consists of 4680 digital optical modules (DOMs) that are able to register light that is scattered and propagated through the ice (more info about these modules can be found in Section 1.2.1). The DOMs are attached to cables and are frozen in the ice. In total, 78 of these “strings” were frozen into boreholes and spread out over a cubic kilometer in a hexagonal shape. Because only the deep ice is transparent, the DOMs are attached to the strings starting from a depth of 1450 meters to 2450 meters. The strings, as viewed from above, are spaced about 125 meters apart and along each string, 60 DOMs are attached with a vertical separation of 17 meters. This design was chosen in order to meet up to the primary science requirement of detecting astrophysical neutrinos in the energy range of $\mathcal{O}(\text{TeV})$ – $\mathcal{O}(\text{PeV})$.

1.1.2 DeepCore

A subset of in-ice DOMs is deployed along eight extra strings in the central region of the in-ice array. The optical modules are deployed deeper than 1750 meter with a denser instrumented volume. Seven additional strings, belonging to the standard in-ice strings, are also combined with the DeepCore strings to optimize the instrumented volume for this detector. The inter-string spacing on the eight specialized DeepCore strings varies from 41 meters to 105 meters. The DOM-to-DOM spacing is 7 meters for the bottom 50 optical modules (which are deployed at depths of 2100 to 2450 meters). The remaining 10 DOMs on each string are located at depths above 2000 meters deep with a spacing of 10 meters. This extra “layer” serves as a veto for downgoing atmospheric muons. Each string is instrumented with 60 DOMs, resulting in a total of 480 DOMs. Instrumentation in the ice between 2000 to 2100 meters proved to be less useful due to the *dust layer* (see Section 1.5) and was therefore left out. Six out of the eight specialized strings are also instrumented with DOMs using PMTs of higher quantum efficiency. The two remaining strings are instrumented with regular IceCube DOMs. A layout of the in-ice array is given in Figure 1.3.

The DeepCore design allows us to detect neutrinos of much lower energies in the range of $\mathcal{O}(10 \text{ GeV})$ – $\mathcal{O}(100 \text{ GeV})$. Experiments for neutrino oscillation experiments, WIMP dark matter annihilation, galactic supernova neutrinos and point sources are made possible, or more feasible, with this dense subarray [150].

1.1.3 IceTop

IceTop is a cosmic ray air shower array, located on the surface of the ice and 2835 meters above sea level. As discussed in Chapter ??, air showers die out when they are propagating to Earth’s surface but as a consequence of the high altitude of IceTop, showers are observed near maximum*, resulting in a good energy resolution for the detector. This is important if one wants to measure changes in composition as a function of energy. In total, 162 ice-filled tanks are distributed in 81 stations (two tanks per station) in a grid similar to the in-ice array. Like the denser DeepCore infill, there are eight stations in the center of IceTop placed more closely together.

The two tanks per station are separated 10 meters apart from each other and each tank contains two IceCube DOMs. One is operated at a “low-gain” and one at “high-gain”, making them more suitable for air shower detection. The tanks measure the Cherenkov light that is produced in the ice of a tank due to the particles in a shower (electrons, positrons, muons and hadrons). The IceTop design allows to fully cover the knee of the energy spectrum and is

*The height of the shower where the maximum number of particles are produced in an air shower is often referred to as the “shower maximum”.

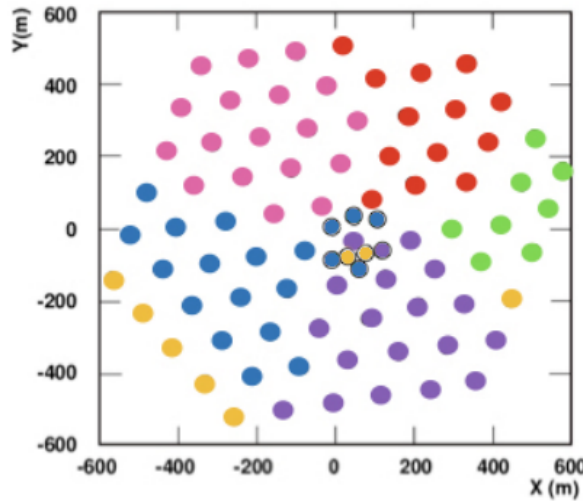


Figure 1.3: Layout of the IceCube (regular) and DeepCore strings (black edge). The string color scheme represents different deployment seasons (04-05: orange, 05-06: green, 06-07: red, 07-08: pink, 08-09: purple, 09-10: blue, 10-11: yellow). Figure from Ref. [151], with minor corrections.

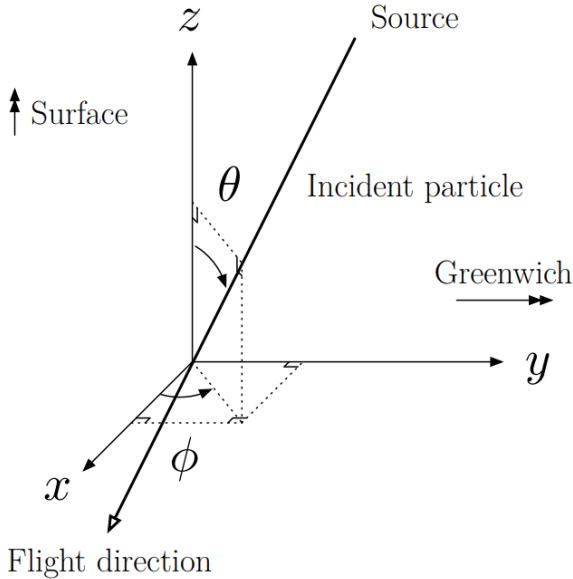


Figure 1.4: The IceCube coordinate system.

primarily sensitive from PeV to EeV energies. The denser infill allows the threshold to be lowered to 100 TeV. The detector is used in studies of the composition, high- p_T muons, etc.

1.1.4 IceCube coordinate system

When referring to positions and directions, one has to define a coordinate system that is able to uniquely define these variables. The system used in the IceCube collaboration is shown in Figure 1.4.

The center of the coordinate system is set close to the geometric center of the detector, at about 2000 m below the surface of the ice. The y-axis of the coordinate system is aligned with the Prime Meridian pointing toward Greenwich (United Kingdom). The x-axis is set perpendicular to the y-axis pointing in a 90° clockwise direction. The z-axis is set perpendicular to the xy-plane, pointing upwards, normal to the Earth's surface.

A particle's direction is defined with zenith and azimuth angles, θ and ϕ respectively. The zenith angle is measured relative to the positive z-axis and the azimuth angle is measured

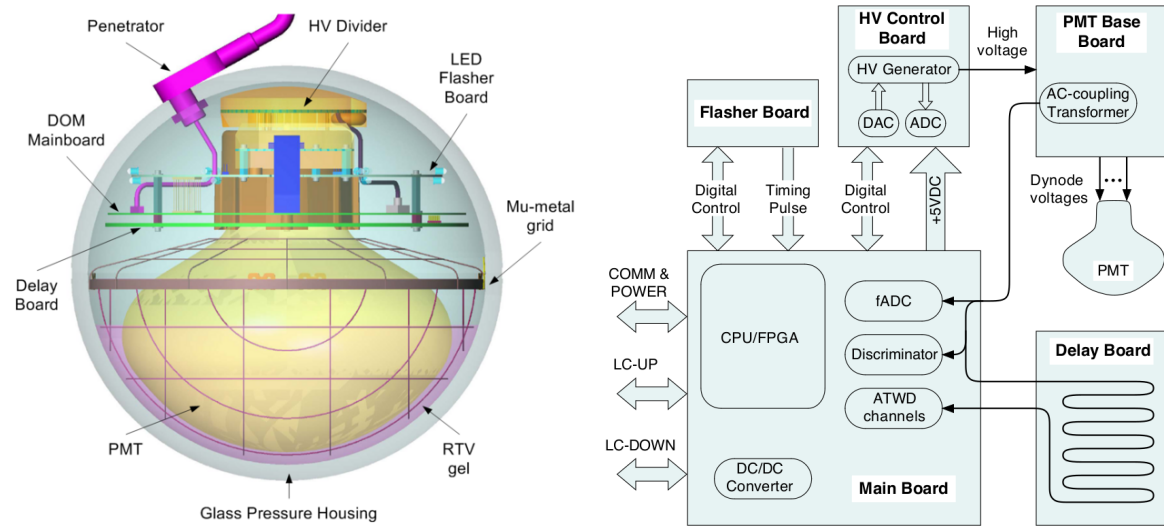


Figure 1.5: *Left:* illustration of the mechanical DOM components. *Right:* Scheme of the functional connections.

counterclockwise from the positive xy-plane.

1.2 Hardware components

1.2.1 Digital optical modules

The Digital Optical Modules, or DOMs, convert light into electrical signals and have the necessary hardware installed to perform some basic processing of the electrical pulses. A downward facing 10"-diameter photomultiplier tube (PMT) is set with a high voltage of 2 kV, resulting in a gain of 10^7 [152]. The amplitude of the resulting waveforms ranges from 1 mV up to and beyond the linearity limit of the PMT (~ 2 V) with the width ranging from 12 ns to 1500 ns. This wide dynamic range of the waveform is processed by onboard electronics: the main board and delay board. The main board controls all the devices in the DOM (high voltage power supply for the PMT, the flasher board and pressure, temperature, and power supply voltage monitor sensors), digitizes the PMT waveforms, communicates with the data acquisition (DAQ) on the surface, houses an internal clock that is regularly calibrated with the DAQ on the surface and exchanges pulses with the adjacent DOMs. An illustration of the mechanical components of the optical module and a schematic view of the data flow starting from the PMT is shown in Figure 1.5. The optical module is housed in a 13"-glass sphere of 0.5" thick made from borosilicate. It is separated into two halves and held together with an aluminium waistband. The sphere was tested up to 690 bar hydrostatic pressure and is able to withstand the enormous pressure that the DOM is exposed to deep within the ice and during freezing (see Section 1.3). A penetrator inside the glass sphere brings out three wires pairs housed in a cable. One wire pair is connected to the string and ultimately to the IceCube Laboratory (see Section 1.2.4), the other two wires to the neighboring DOMs directly above and below for local coincidence pulses (see Section 1.2.3). A detailed description is given in the detector paper [152].

1.2.1.1 PMTs

The 10" (or 25 cm) diameter PMT comes in two types: Hamamatsu R7081-02 for standard IceCube DOMs and a high-quantum-efficiency (HQE) version, Hamamatsu R7081-02MOD for the specialized DeepCore strings [153]. The peak quantum efficiency is around 25% (34% for HQE) at a wavelength of approximately 390 nm. However, the total acceptance of the optical module is the convolution of the quantum efficiency with the glass transmission (93% at 400 nm, decreasing to 50% at 340 nm and 10% at 315 nm at a normal incidence). The resulting acceptance is illustrated in Figure 1.6. The PMTs face downwards and are housed in a mu-metal

grid to shield them from the Earth magnetic field and a silicone gel necessary for optical coupling and mechanical support.

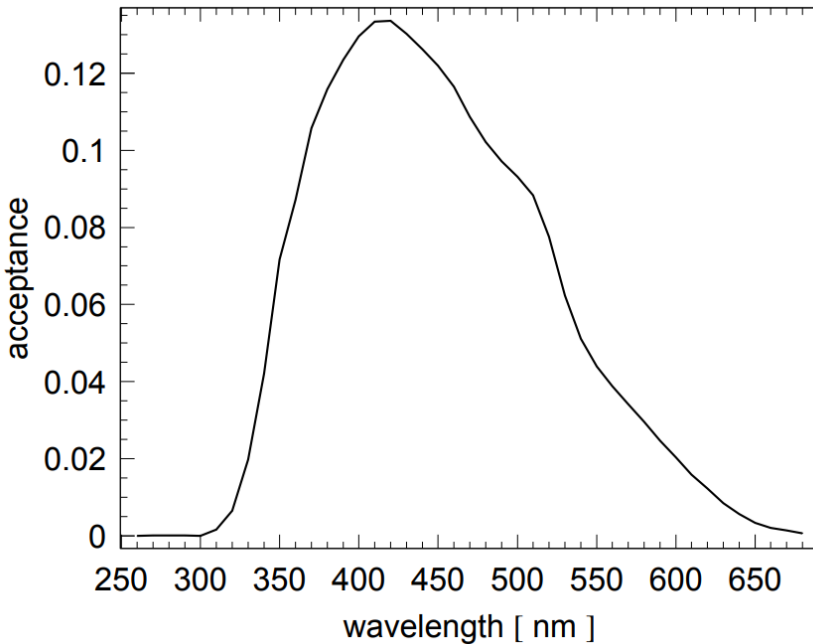


Figure 1.6: Fraction of photons arriving from a direction parallel to the PMT axis in function of the photon wavelength. Glass and gel transmission, PMT quantum and collection efficiencies are all included. Figure from Ref. [154].

1.2.1.2 Main board and delay board

The PMT signals are sent to two ATWD (Analog Transient Waveform Digitizer) and one fast ADC (fADC) with a delay of about 75 ns. This delay is necessary because signals are only processed if the signal exceeds a voltage that corresponds to 0.25 PE (one PE is the voltage that typically corresponds to the voltage produced by a single photoelectron). Once this threshold is crossed, the signal is compressed and included in a “DOMlaunch” or “hit”. Signals that pass the local coincidence requirement (see Section 1.2.3) have their full waveforms compressed, whereas for isolated events only a time stamp and brief charge summary is sent. For each hit, an FPGA (Field Programmable Gate Array) opens up one of the two ATWD chips. Each of the two chips is provided with three amplifier gains with nominal values of 16, 2 and 0.25. Most pulses use the highest-gain channel while the other lower-gain recordings are used as needed when pulses reach 75% of the range of a higher-gain channel. The ATWD recording duration is 427 ns, which should include light that is produced within tens of meters of a DOM. The slower fADC is used when light reaches the DOM after the ATWD time window and samples continuously. The FPGA is programmed to save an interval of 6.4 μ s after the launch. ATWD chips sample the input voltage at 300 Msps, followed by a 10-bit digitization. The fADC captures the information with a 10-bit 40 Msps.

The two sets of ATWD chips are operated alternately in order to reduce deadtime. After 50 ns, the second chip is available to be launched during the digitization step of the first. The digitization procedure is terminated for isolated hits and the ATWD is reset, reducing the DOM dead time.

The delay board consists of a 10 m-long copper trace that delays the signal for 75 ns, necessary to be able to record the full waveform before the discriminator threshold of 0.25 PE is exceeded.

1.2.1.3 Flasher board

To be able to characterize the ice and simulate light propagation, each DOM was instrumented with 12 LEDs that are aimed in six different azimuth angles (with 60° spacing) and along two

different zenith angles. The LEDs were chosen to have a wavelength spectrum centered at around 400 nm to approximate the typical wavelength of detected Cherenkov photons. Flasher data is used for:

- verifying the timing response of the DOMs throughout the analysis software chain;
- measuring the position of the deployed DOMs in ice;
- measuring the optical properties of the ice (see Section 1.5);
- verifying the performance of shower reconstruction algorithms in measuring position, direction and energy.

1.2.2 Calibration

Regular calibration of the components is necessary to be able to convert the DOM waveforms to reliable and comparable physical units. Optical efficiencies of the optical modules were determined in the lab before deployment and are also done *in situ* with calibration procedures.

Some of these procedures do not allow for simultaneous data-taking and are performed as little as possible, without losing significant confidence in the calibration of the devices. For example, in-ice DOMs are calibrated yearly with the DOMCal procedure, whereas global time calibration can be done in parallel with data-taking and is provided by the RAPCal procedure.

As they result in the vast majority of the background hits, *dark noise* needs to be properly understood for low-energy neutrino analyses, supernova searches, and detector simulations. The total rate of dark noise averages at around 560 Hz for in-ice DOMs and 780 Hz for HQE DOMs. The origins of the noise are non-trivial and include electronic noise, thermionic emission, Cherenkov light from radioactive decays, field emission within the PMT, and scintillation/luminescence in the glass of the PMT and pressure sphere. They are simulated with a combination of uncorrelated (Poissonian) noise and a correlated component. The temperature dependence of the noise rate was determined by combining a measured temperature profile of the South Pole ice cap with a fit of the Poissonian expectation of the total dark noise rate to every individual DOM, and was verified in lab measurements. The seasonal variations of the dark noise rates are below 1%, but are tracked over time and updated yearly in a database.

More information about these and other calibration procedures can be found in Ref. [152].

1.2.3 Cable systems

The DOMs are the eyes of the detector, but the cable system connects all the modules together and links them to the readout hardware at the surface. The in-ice cables, 2505 m long, are each connected to 60 DOMs and terminate at a Surface Junction Box (SJB) between IceTop tanks. IceTop tanks also connect to the SJB. A surface cable was trenched 1 m deep at the time of deployment and runs to the IceCube Laboratory. One cable consists of 20 “quads”, a construction of four twisted wires. Four quads provide special instrumentation and local coincidence between connections and one is a spare. The remaining 15 quads are each connected to four DOMs with two wire pairs. A wire pair connects two adjacent DOMs and is attached to connectors at 30 breakouts spaced 34 m apart as can be seen in Figure 1.7. Each DOM is connected to three wire pairs. One wire pair is used for bi-directional communication to the surface and power. The two remaining wires are dedicated to determine *Local Coincidence (LC)*. Each DOM is connected to its nearest neighbor above and below. If nearest or next-to-nearest neighbors are hit within a time window of $\pm 1 \mu\text{s}$, the hits are said to be in Hard Local Coincidence (HLC). Isolated hits are referred to as Soft Local Coincidence (SLC). Most DOM hits originate from dark noise (see Section 1.2.2) and are not in HLC. Light originating from particles traveling through matter is more likely to trigger DOMs in close proximity. Therefore, LC requirements are able to drastically reduce the noise rate.

1.2.4 IceCube laboratory

The central building to which the modules of all the detectors are connected is the IceCube Laboratory (ICL). Cables/strings from the arrays run up two cable towers on either sides of the

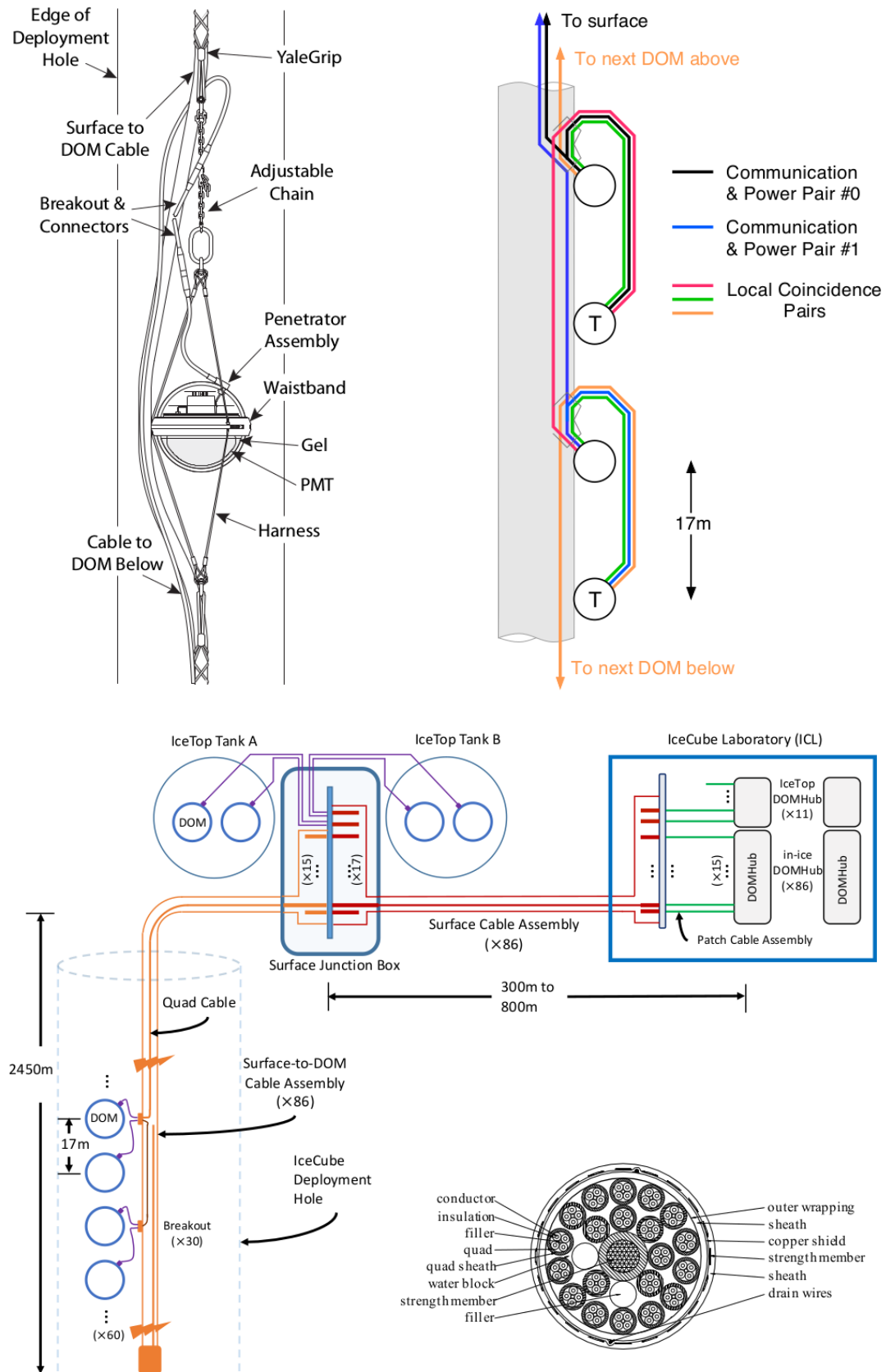


Figure 1.7: *Top:* Sketch of DOM cabling and schematic overview. The modules are connected to their nearest neighbors and the string. *Bottom:* General schematic overview of the IceCube cabling system and the connection between all components together with an in-ice cable cross section. Illustrations from Ref. [152].

structure. A picture of the ICL is shown as the header image of this chapter (pg. 3); one of the towers is visible. Inside the main part of the building is a server room to which the cables in the towers are connected. All data acquisition and online filtering computers are housed inside the server room together with the main IceCube computing system called the “South Pole System” (more information on this in Section 1.4).

1.3 Deployment

In total, 86 holes had to be drilled for all IceCube and DeepCore strings. The surface consists of a 50 m snow and firn region with a gradual transition to ice. The ice was melted with a 5 MW Enhanced Hot Water Drill (EHWD) capable of drilling about 1 hole per 48 hours. The holes were 60 cm in diameter, providing enough clearance for the optical modules that were 35 cm in diameter, and with contingency time for delays that meant holes could shrink due to refreezing. Because melting snow and firn with hot water is not practical, a specialized drill with copper tubing through which hot water flows was used to melt the firn by contact.

The IceCube drilling was completed in seven field seasons during Antarctic summers (early November to mid-January). The first season started in 2004-2005 and construction ended in 2010-2011.

After drilling one hole, all 60 DOMs were lowered one by one and connected to each other with the penetrator assembly as shown in Figure 1.7. After deployment of all DOMs, the remaining 1.5 km of in-ice cable was lowered into the hole (known as the “drop phase”). The top of the cable was then secured by an anchor trenched in the snow and connected to the Surface Junction Box.

In total, 5484 (5160 IC + 324 IT) optical modules were deployed and as of 2018, there are 5396 still in data-taking mode (98.4%). There were 55 DOMs that failed almost immediately during freeze-in, while 34 DOM failures occurred after deployment. This number includes modules on a wire pair that are taken out when the partner DOM on the same pair failed. The mean failure rate is estimated to be around $(4.1 \pm 1.2) \text{ yr}^{-1}$, which results in a survival fraction of $(97.4 \pm 0.3)\%$ in 2030.

1.4 Data taking

First processing of the photon detection is done inside the DOM. After digitization, the waveforms are sent along the cable/string to which all DOMs are attached and that runs to the ICL. Each one of the strings is connected to one of the DOMHubs, which together with servers that run various online systems, comprises the South Pole System (SPS). An overview is given in Figure 1.8.

The data acquisition (DAQ) system is run on the DOMHubs and recognizes patterns in hits that are most likely caused by particle interactions with the use of the implemented triggers and filters (see below). This combination of hits is called an “event”. Most of the DAQ data rate originates from atmospheric muons with an event rate averaging 2.7 kHz. The total bandwidth saved to tape/disk (see Section 1.4.3) is approximately 1 TB/day.

To implement possible changes in the detector settings, triggers, or filters, a full physics run spans over one year, starting in May and ending in May the following year. Data is recorded in smaller 8 hour runs, where each run has a unique run number. Over the years, with the use of both online and on-site automatic alerts, the total uptime of the detector has a steady increase of clean uptime (usable data) from 89.75% in 2011 to 98.89% in 2018.

1.4.1 Triggers

Aside from the discriminator thresholds in the module (see Section 1.2.1.2), a system of triggers is set up to further reduce the noise rate and refine searches for physics events. Below, a short description of the triggers is given. An overview of the trigger settings is given in Table 1.1.

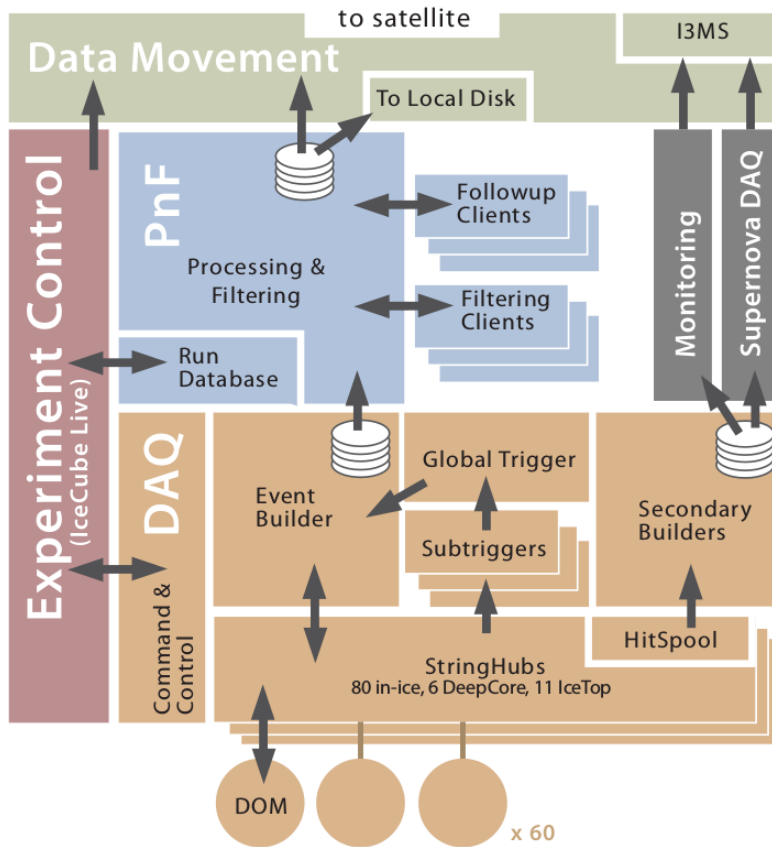


Figure 1.8: Schematic overview of the data flow in the primary IceCube online systems.

- The most important trigger is the Simple Multiplicity Trigger (SMT) used for the IceCube, DeepCore and IceTop arrays. The trigger setting requires a certain number of hits within a time window of the order of a couple of μs without any locality requirements.
- The Volume Trigger requires less HLC hits, but they have to be clustered in a certain cylindrical volume.
- Locality conditions are powerful for low-energy events that do not reach far in the detector but are more prone to produce hits in a small volume and time window. Therefore, a dedicated String Trigger was designed for low-energetic upgoing events passing along a single string.
- IceCube is also sensitive to hypothetical massive particles moving at subrelativistic speeds: magnetic monopoles. Therefore, a dedicated Slow Particle (SLOP) trigger has been developed. It searches for triplets of HLC pairs within a window, T_{\max} , and removes HLC pairs within a time window, T_{prox} , to remove hits originating from particles traveling at the speed of light. Other velocity and geometric requirements are set with the inner angle between triplets, α_{\min} and the “velocity” along the sides of the triangle.
- A Fixed Rate Trigger (FRT) reads out hit data from the full detector at fixed intervals, useful for DOM noise studies.

If a trigger condition is fulfilled, the start of the trigger window is determined as the first HLC hit of the active volume of the trigger. The minimum length of the triggered window slides along with the hits until there is no more HLC after the last hit within the set minimum time window. The length of a triggered set of hits can therefore be longer than the minimum trigger window. As one event is able to fulfill multiple trigger requirements, the (sub)triggers are merged into one Global Trigger while keeping the information on the individual triggers. This data is subsequently sent to the Event Builder that writes DAQ events (also called *Q frames*) to a temporary file that is saved when it reaches a certain size. These events are eventually re-split into physics events (*P*

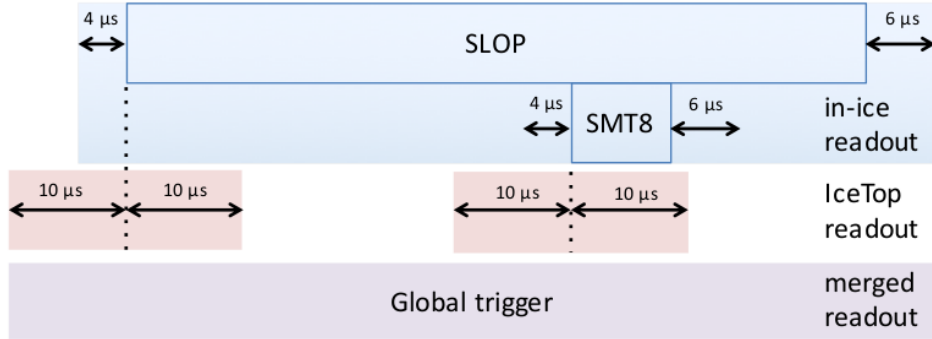


Figure 1.9: Example of a global trigger construction. Multiple triggers are combined due to their overlap with the long SLOP trigger.

Table 1.1: Parameter settings of triggers (as of May 2016) and typical trigger rates.

| Trigger | DOM set | N HLC hits | Trigger Window (μs) | Readout Window (μs) IC | Readout Window (μs) IT | Topology | Rate (Hz) |
|---------|----------|----------------------|----------------------------------|--|--|---|-----------|
| SMT | in-ice | 8 | 5 | -4, +6 | ± 10 | - | 2100 |
| SMT | DeepCore | 3 | 2.5 | -4, +6 | ± 10 | - | 250 |
| SMT | IceTop | 6 | 5 | ± 10 | ± 10 | - | 25 |
| Volume | in-ice | 4 | 1 | -4, +6 | ± 10 | cylinder ($r = 175 \text{ m}$, $h = 75 \text{ m}$) | 3700 |
| Volume | IceTop | 4 | 0.2 | ± 10 | ± 10 | cylinder ($r = 60 \text{ m}$, $h = 10 \text{ m}$) | 4 |
| String | in-ice | 5 | 1.5 | -4, +6 | ± 10 | 7 adjacent vertical DOMs | 2200 |
| SLOP | in-ice | N_{triplet} | $T_{\text{prox}} = 2.5$ | $-4, +6$ | ± 10 | $\alpha_{\min} = 140^\circ$, $v_{\text{rel}}^{\max} = 0.5$ | 12 |
| | | | $T_{\min} = 0$ | | | | |
| | | | $T_{\max} = 500$ | | | | |
| FRT | all | - | - | Combined: 10000 | - | - | 0.003 |

frames) corresponding to a certain subtrigger before reconstruction and analysis. An example of a Global Trigger, here mostly determined by the very long SLOP trigger, is shown in Figure 1.9.

All triggers read out all SLC/HLC hits of all DOMs, even the ones not directly involved in the trigger construction. For this, they use the StringHub software component located on every DOMHub that is able of caching SLC and HLC hits in memory. Hits before and after the trigger window are also saved to the event to add information of early and late pulses. This is typically 4 μs before and 6 μs after the trigger window for in-ice triggers.

1.4.2 Filters

Events are sent through the online Processing and Filtering (PnF) system for additional processing. First, the triggered events have their waveforms further compressed using the Super Data Storage and Transfer format (SuperDST), which uses only 9% of the storage size of the full waveform information. Very fast, basic reconstructions are run on the SuperDST waveforms to compute the vertex position, energy, direction and goodness-of-fit that are necessary for the filter selections of possible interesting events.

Around 25 filters search for a wide range of different types of particle interactions, ranging from low-energy neutrinos for oscillation measurements to the highest-energy neutrino interactions illuminating large parts of the detector. Some filters are designed to look for neutrino events of wide astrophysical interest to the scientific community and trigger alerts that are distributed to followup observatories worldwide. One example is the “EHE alert” that searches for Extremely High Energy neutrinos that are most likely of astrophysical origin [155]. Another example is the Gamma Follow Up alert that notifies the MAGIC and VERITAS collaborations when significant bursts of neutrinos from known high-energy gamma-ray sources over periods up to 3 weeks occur [156]. Other filters look for events that could be caused by muons, WIMPs, monopoles, etc. The filters that were used in this analysis are given in Section ??.

As a bonus, filtering reduces the data volume to a level of around 90 Gb/day, which is small enough to transfer to the North using a satellite.

1.4.3 Data handling

Most of the data is processed with the PnF system. The geometry, calibration, and detector status (GCD) information from each 8 hour run is sent via the same satellite transfer that is used for the continuously running PnF system. All the raw waveforms were written to tape before that system was retired in 2015. Since then, disks have been used to store the remaining archival data. This raw data is shipped to the North every year and is used if reprocessing of data is necessary. An example is the SPE correction for all runs starting from 2010 to 2016 referred to as *pass2 data* [157].

Files are stored in IceCube specific files and are called *i3files*.

1.5 Antarctic ice

The ice, in which the optical modules are frozen, acts as the propagation medium for the light that is produced by relativistic particles. Therefore, the parameterization of the ice is of great importance for good reconstructions and reliable simulations. The relativistic particles that travel through the ice produce photons in a Cherenkov cone of around 41° (see Section ??). How these photons further propagate from the point of emission to the receiving sensors is determined by the absorption and scattering within the ice. The most important parameters necessary to describe the photon propagation in ice are:

- the average distance to absorption,
- the average distance between successive scatters of photons, and
- the angular distribution of the new direction of a photon at each given scattering point.

There has been a large effort into measuring and modeling the Antarctic ice that is still ongoing. A good summary (although is a bit outdated as it does not include ice anisotropy effects, cable shadowing and DOM tilts) can be found in Ref. [154].

1.5.1 Ice simulation

The ice is modeled by the six-parameter ice model introduced in Ref. [158]. Flasher data from LEDs is used to fit the model to data (see Section 1.2.1.3). In this model, the ice is described by a table of depth-dependent parameters $b_e(400)$ and $a_{dust}(400)$ related to scattering and absorption at a wavelength of 400 nm. These two parameters depend on the relative temperature $\delta\tau$, which changes in function of depth, and six global parameters. The effective scattering coefficient is equal to $b_e = b \cdot (1 - \langle \cos \theta \rangle)$, where b is the geometrical scattering coefficient that determines the average distance between successive scatters and θ is the deflection angle at each scatter. The absorption coefficient a determines the average distance traveled by a photon before it is absorbed and is the sum of two components: one due to dust and the other a temperature dependent component for pure ice.

$$b_e(\lambda) = b_e(400) \cdot \left(\frac{\lambda}{400} \right)^{-\alpha}, \quad (1.1)$$

$$a(\lambda) = a_{dust}(\lambda) + Ae^{-B/\lambda} \cdot (1 + 0.01 \cdot \delta\tau), \quad (1.2)$$

with $a_{dust}(\lambda) = a_{dust}(400) \cdot \left(\frac{\lambda}{400} \right)^{-\kappa}$.

α, κ, A and B are determined in Ref. [158]*, $\delta\tau$ is equal to

$$\delta\tau(d) = T(d) - T(1730\text{m}), \quad (1.3)$$

with $T(d) = 221.5 - 0.00045319 \cdot d + 5.822 \cdot 10^{-6} \cdot d^2$,

*The remaining two parameters D and E were not used here.

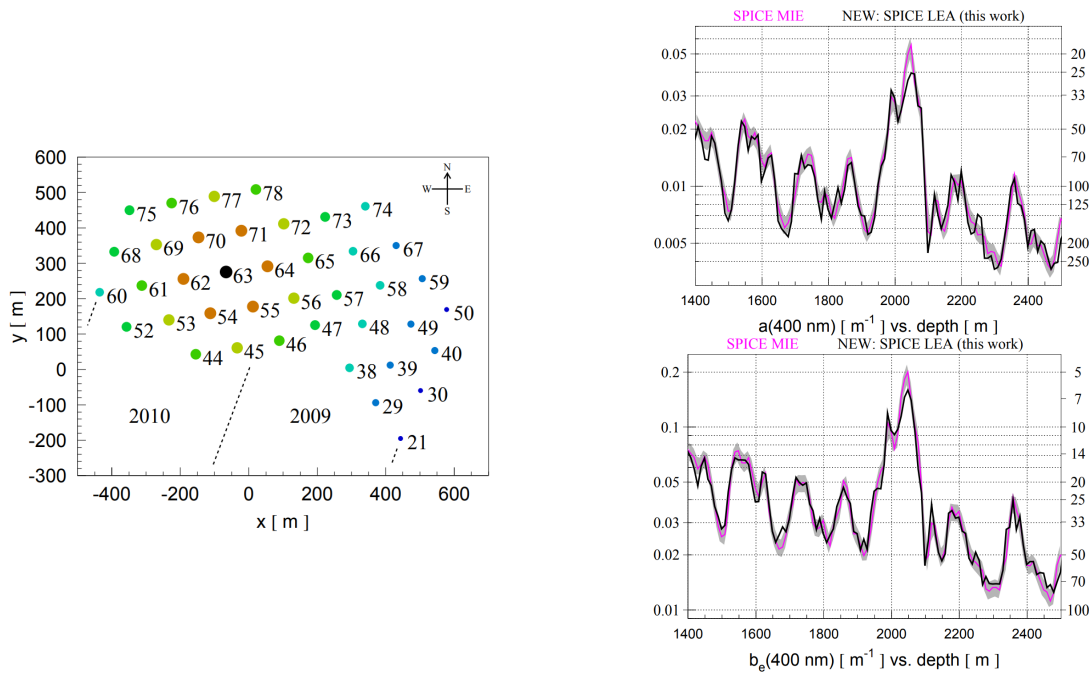


Figure 1.10: *Left:* Top view of the 2008 detector configuration when DOMs on string 63 were used to flash LEDs in a flasher run. Same colors are used for strings located at a similar distance to the central string. *Right:* values of $b_e(400)$ and $a(400)$ vs. depth for two different ice models. The scale and numbers to the right of each plot indicate the corresponding effective absorption $1/a$ and scattering $1/b_e$ lengths in [m]. Both illustrations from Ref. [159].

where d is the relative depth compared to the center of AMANDA (1730 m depth). Using flasher data with 400 nm wavelengths, it is possible to measure the values of $b_e(400)$ and $a_{dust}(400)$ at certain depths and use the six-parameter ice model to extrapolate scattering and absorption for other wavelengths.

In 2008, a flasher run was launched where each DOM on string 63 was producing flashes. The layout of the detector at the time of the flasher run and results of fits to $b_e(400)$ and $a(400)$ vs. depth can be found in Figure 1.10. At a depth between 2000 meters and 2100 meters, a large increase in scattering and absorption is clearly visible. A *dust layer*, presumably originating from volcanic ash, is characterized by an increase of dust in the ice, responsible for the higher scattering and absorption factors.

Over the years, multiple different ice models have been constructed. For this analysis the SPICELea* model has been set as nominal. This is the most recent model that has significant Monte Carlo background simulations available. It includes an angular sensitivity estimation due to the *hole ice*, a column of ice approximately 30 cm in radius immediately surrounding the strings with an increased amount of scattering. More information about this model can be found in Ref. [159].

1.5.2 Systematic uncertainties

The characteristics of the ice are complex. Dust particles, the tilt in the ice sheets, etc. result into non-negligible uncertainties in the ice model. Data from the flasher runs are compared to simulation and this verification was used to quantify the uncertainty on the measured values of $b_e(400)$ and $a(400)$. From this, it was determined that $(+10\%, 0), (0, +10\%)$ and $(-7.1\%, -7.1\%)$ uncertainties on the scattering and absorption coefficients, respectively, was a conservative estimation.

*SPICE stands for South Pole Ice. Lea is an addition to distinguish the different model types, but has (as far as the author knows) no special meaning.

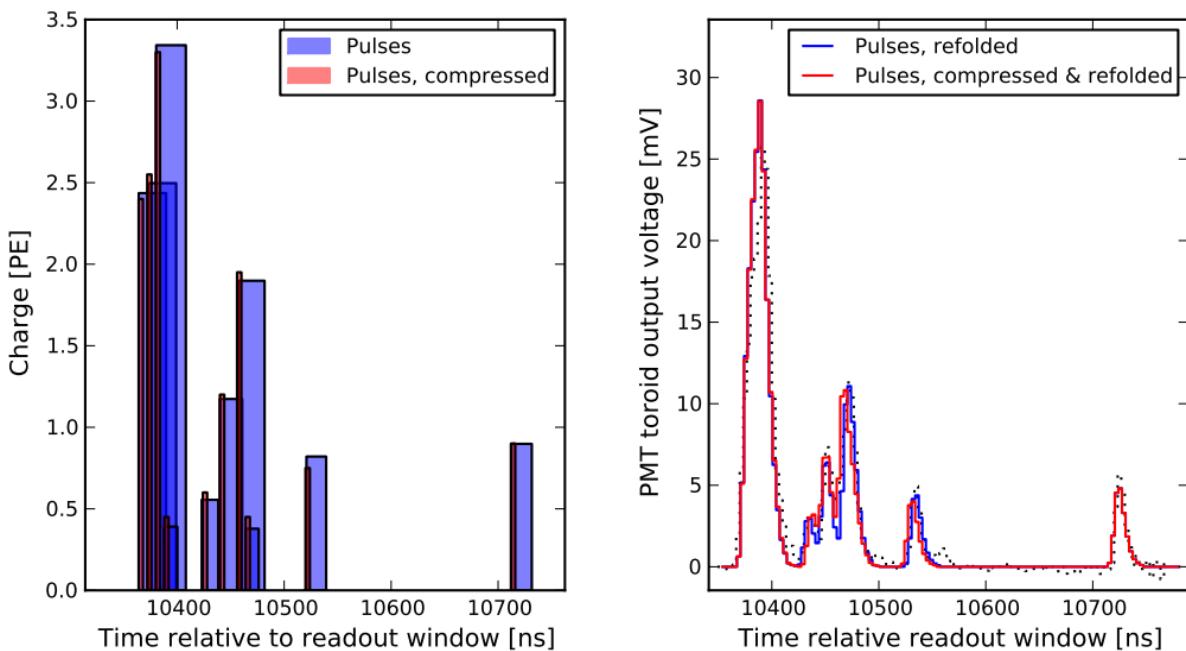


Figure 1.12: *Left:* pulse information illustrated with blue bars; the leading-edges time, width, and charge of the pulse are given by the left edge, width, and height of the bar, respectively. The red bars show the same after SuperDST compression. *Right:* Reconstructed pulses using the full pulse profiles in blue are compared to an approximation of the original waveform that is obtained by convolving the pulse times and charges with an average single-photoelectron pulse shape. Figures from Ref. [160].

1.6 IceCube event topology

The compressed waveforms are refolded to approximations of the original waveforms using average single-photoelectron pulse shapes as can be seen in Figure 1.12. The timing, shape and amplitude of the reconstructed waveforms in all the DOMs in an event are used to characterize the event topologies in the detector. Different interactions give rise to several possible signatures in the detector. Energetic muons propagate several hundreds of meters in the ice and give rise to tracks, whereas electrons and hadrons are stopped almost immediately, giving rise to cascades (see Section ??).

The track-like events, originating from charged-current muon neutrino interactions, provide an angular resolution at a typical angle of 1° for well-contained and reconstructed tracks at 1 TeV and improves to $\sim 0.3^\circ$ for neutrinos with an energy of 1 PeV [161]. Cascades, originating from electromagnetic or hadronic cascades, result in a more spherical light generation in the detector. Well-contained shower events have an average deposited energy resolution of around 15%. These event types are shown in more detail in Figure 1.13.

1.7 Future upgrades

The last couple of years there has been a large focus on improving the physics work that can be done in the IceCube experiment. Several projects are in the pipeline, are under R&D, and/or have been funded to improve the full analysis case of the detector(s).

Lower-energy neutrinos can be detected with a denser infill with other optical modules (the Upgrade, see Section 1.7.1), cosmic ray measurements can be improved with a complementary scintillator array to the IceTop tanks [163] and small air cherenkov telescopes [164]. Also, the detection of ultra-high-energy neutrinos could be made possible with a larger infill of the current IceCube in-ice array (Gen2) or radio antennas. Below a brief summary of projects that could be of potential importance to this analysis is given.

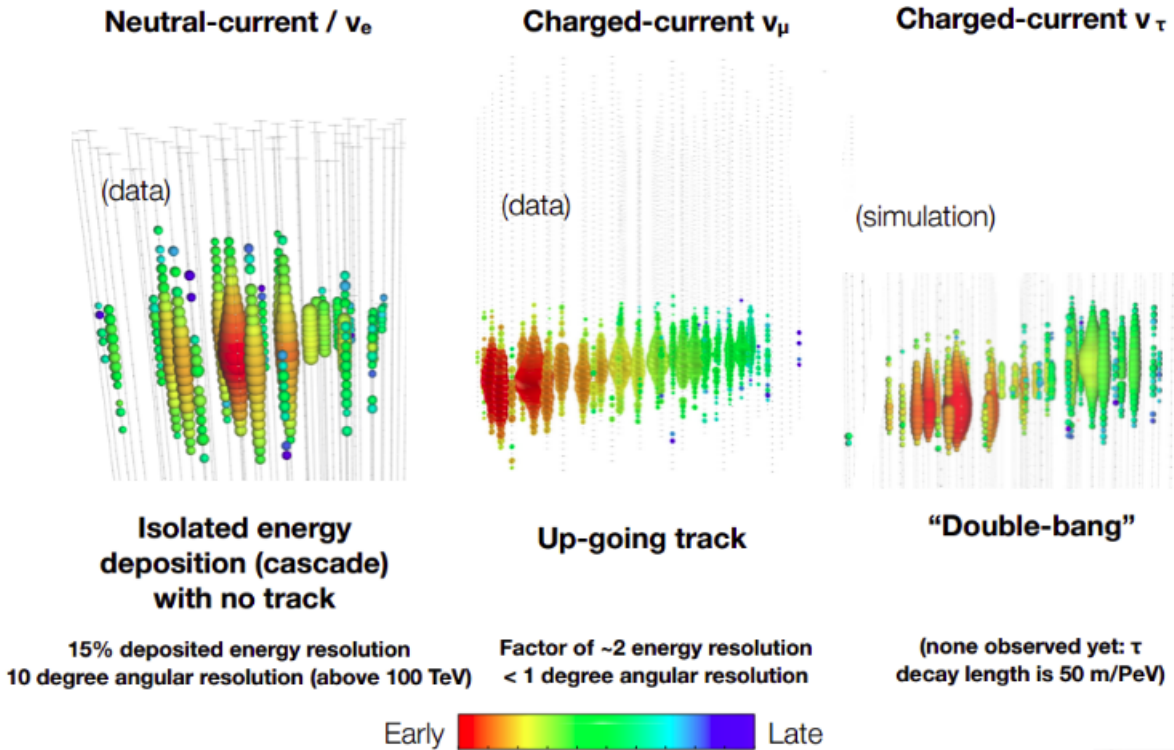


Figure 1.13: Neutrino interactions in the IceCube detector have two distinct types of interactions: cascades and tracks. Energetic taus are theorized to have double-bang signatures but have not undeniably been seen. Colors determine the timing of hits in the optical modules in the ice. Illustrations from the IceCube collaboration [162].

1.7.1 IceCube Upgrade

In 2018, a funding proposal for a dense 7-string infill of DeepCore was accepted by the NSF and was effective from the beginning of October later that year. This infill would have DOMs separated 2.4 m apart and start from a depth of 2140 m, reaching to 2440 m deep in the ice along seven new strings (see Figure 1.14). This very dense array would allow low-energy and oscillation experiments to reach much better sensitivities. Also, very dim tracks such as the ones from particles with an anomalous charge lower than e , might be easier to distinguish from low-energy muons that produce more Cherenkov light.

Because this project involves a restart of the drill, it also serves as a testbed for new optical modules. The Upgrade is the first step towards the much bigger Gen2 project. New types of optical modules would be used with higher angular acceptances than the currently used DOMs that have one large downward facing PMT. Examples are D-Eggs, which have two PMTs at each end of an ellipsoid glass [165], and mDOMs, where multiple smaller PMTs are positioned in a ball-shaped optical module [166].

A camera system could also be included in the new optical module designs and should help to improve the properties of the ice after refreezing [167]. Another camera system, the Precision Optical Calibration Module (POCAM) should further improve our understanding of the ice characteristics and accurately determine the efficiency and angular acceptance of the IceCube DOMs [168].

Deployment is currently planned for the 2022/2023 season.

1.7.2 IceCube Gen2

Although the IceCube in-ice array has successfully been able to determine the flux of astrophysical neutrinos and show the detection of a coincident neutrino with a blazar in an active state, a next generation larger detector infill would greatly improve the detection possibilities of astrophysical

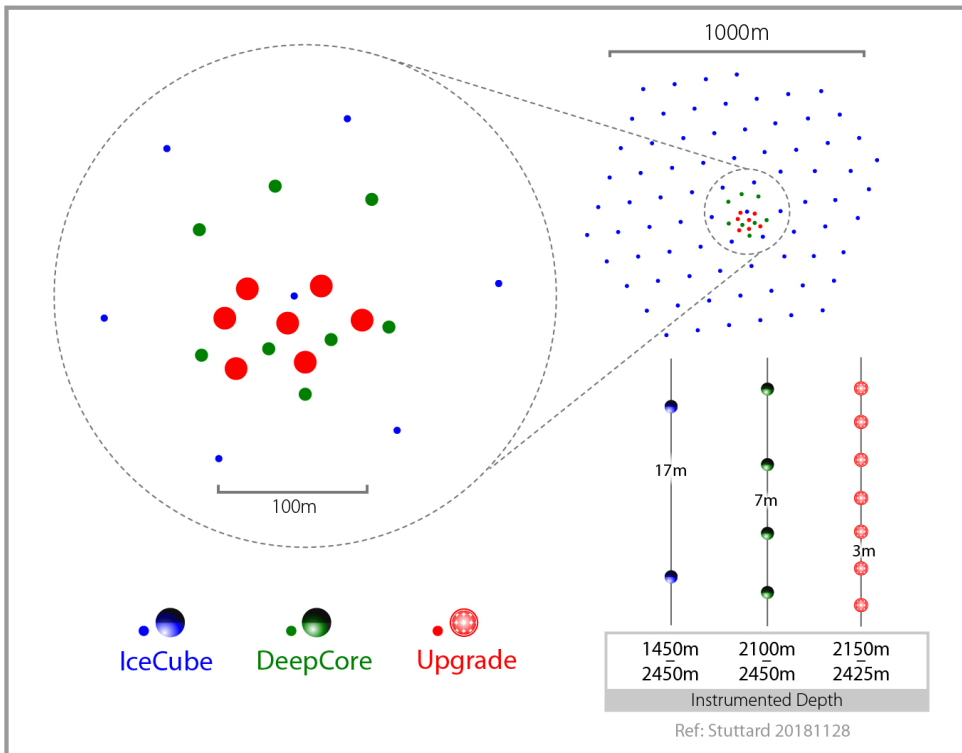


Figure 1.14: Top view of the Upgrade infill (red circles) within the DeepCore array (green) and the whole IceCube detector (blue). The area of the circles is representative of the instrumented photocathode density on a given string. Illustration from the IceCube collaboration.

neutrinos [169]. A 10 km^3 volume of clear glacial ice would allow for a much higher detector acceptance of high-energy neutrino interactions, helping in searches for point sources, better characterizing the spectral and flavor properties, and search for cosmogenic neutrinos among others. Point sources and cosmogenic neutrinos have, for now, not been observed even though the detector has been running stable for a couple of years. There is also only a small set of unambiguous astrophysical neutrinos. It would take extremely large running operations from the current detector (without hardware failures that are prone to happen more and more) to gather enough events for meaningful statistics. A much larger instrumented volume, such as the one proposed, is predicted to have an increase in sensitivity to transient source densities and rated by about two orders of magnitude [170]. Also, a large extension of the active volume could help to look for long tracks originating from SMPs. Although much is undecided, the plans are to have an extra surface array for cosmic ray detection and a radio array for the highest energy neutrinos along the in-ice array.

Deployment is planned for ???

1.7.2.1 In-ice infill

The current design for the Gen2 string configuration would be ~ 120 cables with an inter-string spacing around 250 m to 300 m. This much coarser spread of strings will result in a loss of sensitivity for neutrino events of the order of couple of TeV but would not affect the measurements of the very energetic astrophysical neutrinos. Measurements of the absorption lengths in function of the depth in the ice indicate that the instrumentation of the strings could be extended with an additional 250 m in total. This total depth is comparable to the current depth of the IceCube detector, meaning the surface area should reach to an exposed area of $\sim 10 \text{ km}^2$. This would result in a drastic sensitivity improvement of (near-)horizontal muons traversing the ice that are too energetic to be contained in the current detector.

The IceCube Gen2 Facility

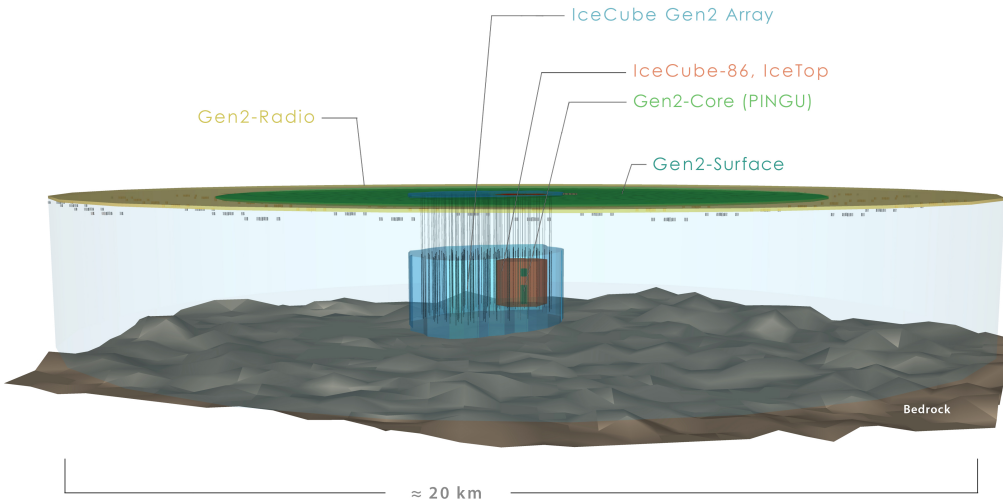


Figure 1.15: Impression of the possible Gen2 layout. The current IceCube in-ice and IceTop arrays are shown in red/brown. The 10x larger Gen2 in-ice array is given in blue. Possible layouts for the radio array (yellow) and surface array (green) are also listed. From the IceCube collaboration. PINGU zit hier bij, maar nog geen idee of dat er van ga komen of dat het bij de upgrade gaat blijven...

1.7.2.2 Surface array

The size of the IceTop array is too limited for most analyses to be used as a veto for most analyses. Therefore, the prospects of a surface array for the Gen2 extension would have much larger designs [171]. The geometry and optimal type of detector that should be used for this configuration is still under design.

1.7.2.3 Radio array

To achieve an improved sensitivity to neutrinos in the $10^{16} - 10^{20}$ eV energy range, including GZK neutrinos, an additional radio-pulse neutrino detector could be constructed. At the critical energy of around 100 PeV, the origins of cosmic rays transitions from the highest-energy galactic sources to the even more extragalactic cosmic rays. A good review of radio emission from cosmic rays is given in Ref. [172]. There are ongoing experiments that act as a proof-of-principle for the radio technique in the ice: ARA (Askaryan Radio Array) [173], close to the IceCube detector at South Pole (see Figure 1.2) and ARIANNA (Antarctic Ross Ice Shelf Antenna Neutrino Array) [174] on the Ross Ice Shelf at the antarctic coast.

1.8 Beyond the Standard Model searches

The IceCube experiment consists of about 300 people from 50 institutions spread over 12 countries. A wide variety of senior scientists, graduate students, technicians, software specialists and engineers works on the continuous running operations to keep the detector running in both hardware and software. Most other people focus on physics analyses that range from low-energy oscillation physics to the rare highest-energy neutrino interactions in the ice. Below I give a general and very brief overview of some IceCube analyses that search for beyond-the-Standard-Model physics.

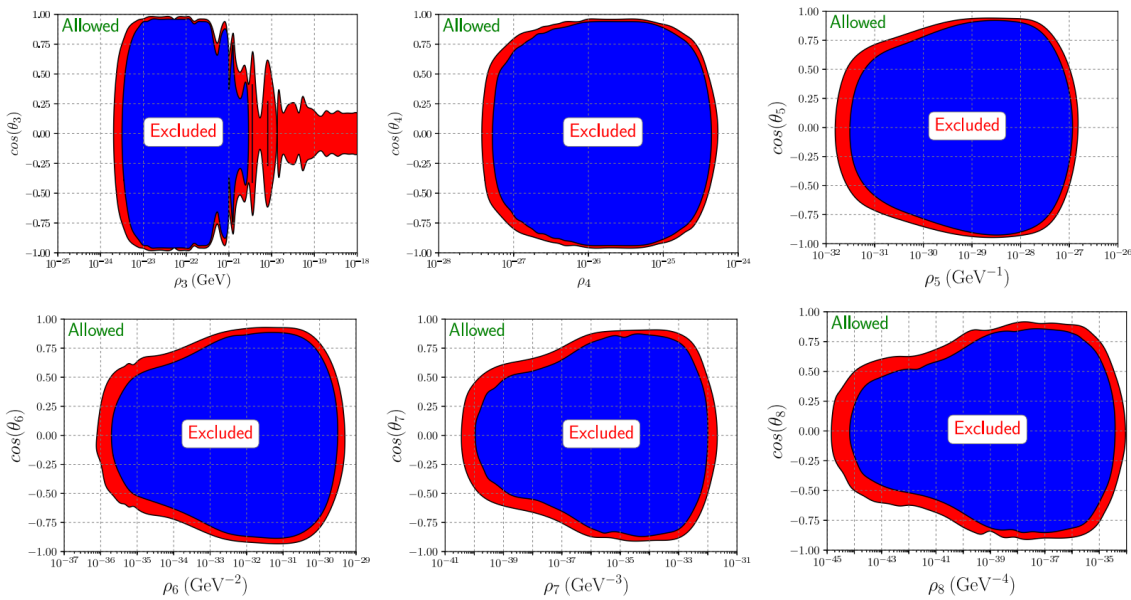


Figure 1.16: Regions excluded at 90% (99%) C.L. in the LIV parameter space in red (blue). ρ is related to the strength of the LIV and $\cos(\theta_d)$ is a combination of coefficients defining LIV in the effective Hamiltonian of Standard Model Extension [175]. The subscript d refers to the power of the corresponding operator in the Hamiltonian. More information in Ref. [176].

1.8.1 Lorentz invariance violation

is dit nu goed uitgelegd of niet?

Lorentz symmetry is one of the foundations of the SM: fundamental laws in nature are thought to be independent of the observer's inertial frame. Some SM extensions allow for spontaneous breaking of Lorentz symmetry and can lead to Lorentz-invariance violating (LIV) effects. Examples are string theory or quantum gravity. Some effects that would follow from these extensions are incorporated in the Standard Model Extension (SME) [175] and although the size of LIV effects should be suppressed by the Planck scale ($\approx 10^{19}$ GeV). They could manifest themselves in, e.g., oscillations of atmospheric neutrinos that would modify the observed energy and zenith angle distributions of atmospheric muon neutrinos observed by the IceCube experiment. The LIV effects are often parametrised by two parameters: ρ_d and $\cos(\theta_d)$ (which are explained in the capture of Figure 1.16), where d refers to the power of the operator in the Hamiltonian. The energy reach of the IceCube detector makes it possible to go to dimensions up to 8 whereas most other experiments are sensitive up to dimension $d = 3$ or $d = 4$. This analysis was done first in the 40-string configuration [177] and later redone with the full detector configuration [176]. Results for $3 \leq d \leq 8$ are shown in Figure 1.16.

1.8.2 Dark matter

The large amount of evidence to support the existence of dark matter (DM) was given in Section ???. Many ongoing experimental efforts try to search for these elusive particles*. Collider experiments try to produce these particles by SM interactions (*production searches*), other experiments try to measure their interaction with SM particles through nuclear recoil (*direct detection*). It should also be possible to search for the SM products that are produced when annihilation of DM occurs and the corresponding daughter particles find their way to Earth (*direct detection*). Most searches focus on specific regions in the sky that are more prone to produce a measurable signal. As one characteristic of DM is its non-zero mass, they are expected to be gravitationally trapped in the halo of galaxies or to accumulate in heavy celestial objects nearby such as the Sun or the Earth itself. Since most SM particles never reach us, neutrinos are the only possible messengers. Figure 1.17 shows a comparison of upper limits on $\langle \sigma_A v \rangle$ versus

*Assuming that they are in fact particles.

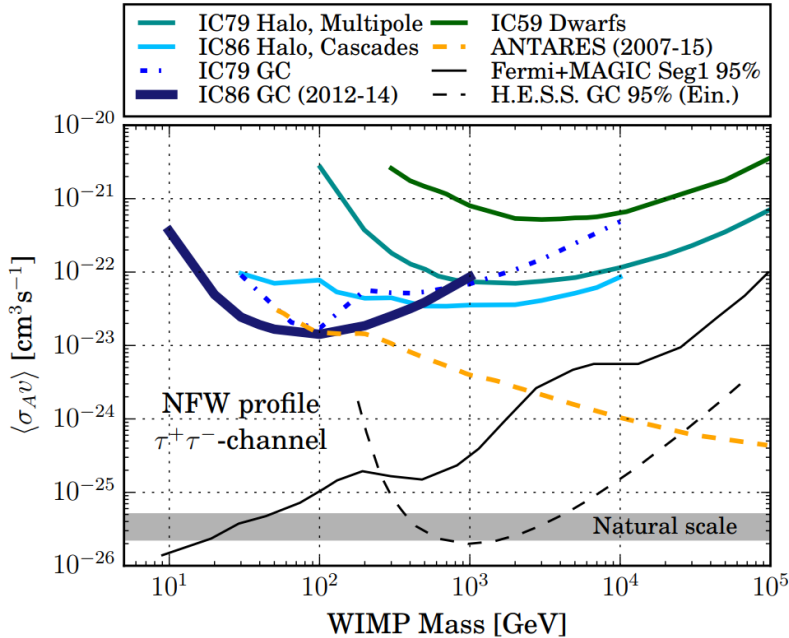


Figure 1.17: Upper limits of $\langle\sigma_A v\rangle$ in function of the WIMP mass from different experiments.

WIMP mass*, for the annihilation channel $\chi\chi \rightarrow \tau^+\tau^-$ producing tau neutrinos. $\langle\sigma_A v\rangle$ is the WIMP-WIMP annihilation cross section and determines the strength of the expected neutrino flux. The analysis mentioned in the figure searched for signals from the center of the Milky Way [178]. Other IceCube analyses have searched for dark matter in the Sun [179, 180] and in the Earth [181].

1.8.3 Magnetic monopoles

The quantum theory of magnetic charge started with a paper by P. Dirac [182] in which he theorized the existence of magnetic monopoles in a similar fashion as he did to successfully predict the positron. If q_m is the magnetic charge and q_e the electric charge, Dirac found that the following condition should hold

$$q_m q_e = 2\pi n \quad (n \in \mathbb{Z}), \quad (1.4)$$

and could therefore explain why the electric charge is always quantized, i.e. in integer multiples of an elementary charge. The smallest possible magnetic charge would be*

$$g_D = 2\pi/e = e/2\alpha \approx 68.5e, \quad (1.5)$$

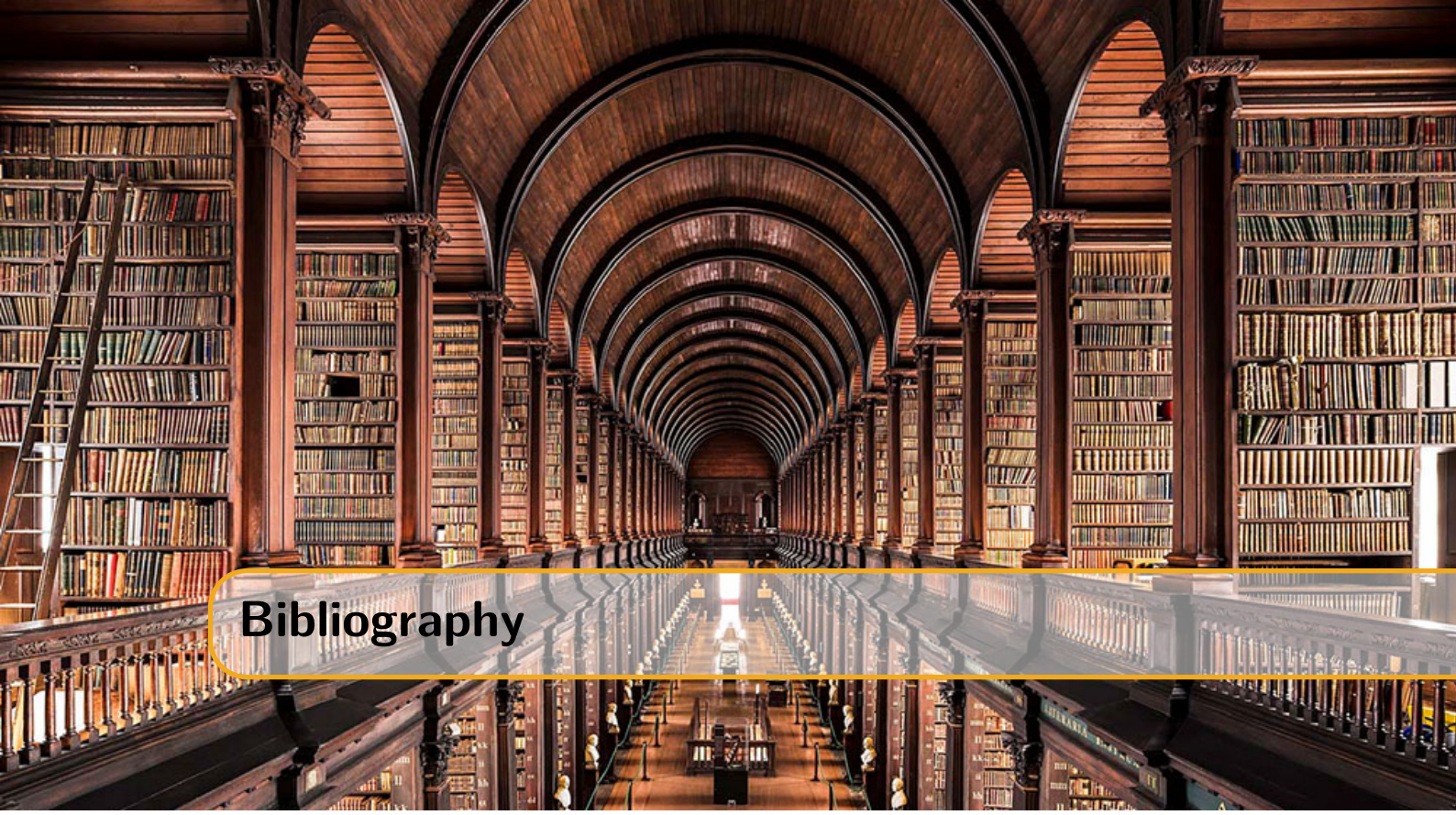
with $\alpha = e^2/\pi$ in natural units. Magnetic monopoles appear automatically in certain Grand Unified Theories that would give rise to these particles after spontaneous symmetry breaking of the GUT group, similar to the Higgs mechanism [183, 184]. Masses are typically of the order of 10^{16-17} GeV. They are searched for in IceCube analyses in multiple velocity ranges. Monopoles with velocities close to the speed of light in vacuum produce extremely bright tracks due to their high Dirac charge as shown in Eq. 1.5. At lower velocities ($\approx 0.5c$ to $0.76c$) secondary knock-off δ -electrons could have velocities above the Cherenkov threshold and produce light. Luminescence light from excitation of the ice dominates at low relativistic velocities ($\approx 0.1c$ to $0.5c$). For each of these speed ranges, searches for magnetic monopoles at the IceCube experiment are either in progress (luminescence) or have already set the world's best upper limits on the flux of magnetic monopoles over a wide range of velocities [185].

*WIMP stands for Weakly Interacting Massive Particle and is one possible candidate for dark matter.

*At the time of writing his paper, Dirac believed the smallest electric charge was from the electron. Since now we know the down quark holds an electric charge equal to $1/3e$, the minimal magnetic charge would be equal to $3g_D$.

1.9**Discussion**

Nodig om over te gaan van deel 1 naar deel 2? Zou zeggen van wel. Kort.



Bibliography

- [1] B. Povh et al. *Particles and nuclei: An Introduction to the physical concepts*. 1995. DOI: 10.1007/3-540-36684-9.
- [2] Michael E. Peskin and Daniel V. Schroeder. *An Introduction to quantum field theory*. Reading, USA: Addison-Wesley, 1995. ISBN: 9780201503975, 0201503972. URL: <http://www.slac.stanford.edu/~mpeskin/QFT.html>.
- [3] M. Tanabashi et al. “Review of Particle Physics”. In: *Phys. Rev. D* 98 (2018), page 030001.
- [4] Alessandro Bettini. *Introduction to elementary particle physics*. 2008. ISBN: 9780521880213. URL: <http://www.cambridge.org/catalogue/catalogue.asp?isbn=9780521880213>.
- [5] CERN. URL: <https://home.cern/about/physics/standard-model>.
- [6] Arthur B. McDonald. “Nobel Lecture: The Sudbury Neutrino Observatory: Observation of flavor change for solar neutrinos”. In: *Rev. Mod. Phys.* 88 (3 July 2016), page 030502. DOI: 10.1103/RevModPhys.88.030502. URL: <https://link.aps.org/doi/10.1103/RevModPhys.88.030502>.
- [7] CMS. URL: <http://cms.web.cern.ch/news/jets-cms-and-determination-their-energy-scale>.
- [8] A. Kircher. *Athanassii Kircherii... Magnes, sive De arte magnetica opus tripartitum...* sumptibus H. Scheus, 1641. URL: <https://books.google.be/books?id=1aZ3FcTAYdUC>.
- [9] G. Farmelo. *The Strangest Man: The Hidden Life of Paul Dirac, Mystic of the Atom*. Basic Books, 2009. ISBN: 9780465019922. URL: <https://books.google.be/books?id=q sodmIGD0fMC>.
- [10] F. Mandl and G. Shaw. *Quantum Field Theory*. Wiley, 2013. ISBN: 9781118716656. URL: <https://books.google.be/books?id=jTBzQfctvHAC>.
- [11] Flip Tanedo. URL: <https://www.quantumdiaries.org/2012/02/14/why-do-we-expect-a-higgs-boson-part-ii-unitarization-of-vector-boson-scattering/>.
- [12] S. L. Glashow, J. Iliopoulos, and L. Maiani. “Weak Interactions with Lepton-Hadron Symmetry”. In: *Phys. Rev. D* 2 (1970), pages 1285–1292. DOI: 10.1103/PhysRevD.2.1285.
- [13] J. H. Christenson et al. “Evidence for the 2π Decay of the K20 Meson”. In: *Physical Review Letters* 13 (July 1964), pages 138–140. DOI: 10.1103/PhysRevLett.13.138.

- [14] Ziro Maki, Masami Nakagawa, and Shoichi Sakata. “Remarks on the Unified Model of Elementary Particles”. In: *Progress of Theoretical Physics* 28.5 (1962), pages 870–880. DOI: 10.1143/PTP.28.870. eprint: /oup/backfile/content_public/journal/ptp/28/5/10.1143/ptp.28.870/2/28-5-870.pdf. URL: <http://dx.doi.org/10.1143/PTP.28.870>.
- [15] Claudio Giganti, Stéphane Lavignac, and Marco Zito. “Neutrino oscillations: the rise of the PMNS paradigm”. In: *Prog. Part. Nucl. Phys.* 98 (2018), pages 1–54. DOI: 10.1016/j.ppnp.2017.10.001. arXiv: 1710.00715 [hep-ex].
- [16] C. D. Anderson. “The Positive Electron”. In: *Phys. Rev.* 43 (1933), pages 491–494. DOI: 10.1103/PhysRev.43.491.
- [17] Paul A. M. Dirac. “The quantum theory of the electron”. In: *Proc. Roy. Soc. Lond.* A117 (1928), pages 610–624. DOI: 10.1098/rspa.1928.0023.
- [18] S. H. Neddermeyer and C. D. Anderson. “Note on the Nature of Cosmic Ray Particles”. In: *Phys. Rev.* 51 (1937), pages 884–886. DOI: 10.1103/PhysRev.51.884.
- [19] C. M. G. Lattes et al. “PROCESSES INVOLVING CHARGED MESONS”. In: *Nature* 159 (1947). [,42(1947)], pages 694–697. DOI: 10.1038/159694a0.
- [20] F. J. Hasert et al. “Observation of Neutrino Like Interactions Without Muon Or Electron in the Gargamelle Neutrino Experiment”. In: *Phys. Lett.* B46 (1973). [,5.15(1973)], pages 138–140. DOI: 10.1016/0370-2693(73)90499-1.
- [21] G. Arnison et al. “Experimental Observation of Isolated Large Transverse Energy Electrons with Associated Missing Energy at $s^{**}(1/2) = 540\text{-GeV}$ ”. In: *Phys. Lett.* B122 (1983). [,611(1983)], pages 103–116. DOI: 10.1016/0370-2693(83)91177-2.
- [22] G. Arnison et al. “Experimental Observation of Lepton Pairs of Invariant Mass Around 95-GeV/c $^{**}2$ at the CERN SPS Collider”. In: *Phys. Lett.* B126 (1983). [,7.55(1983)], pages 398–410. DOI: 10.1016/0370-2693(83)90188-0.
- [23] S. W. Herb et al. “Observation of a Dimuon Resonance at 9.5-GeV in 400-GeV Proton-Nucleus Collisions”. In: *Phys. Rev. Lett.* 39 (1977), pages 252–255. DOI: 10.1103/PhysRevLett.39.252.
- [24] F. Abe et al. “Observation of top quark production in $\bar{p}p$ collisions”. In: *Phys. Rev. Lett.* 74 (1995), pages 2626–2631. DOI: 10.1103/PhysRevLett.74.2626. arXiv: hep-ex/9503002 [hep-ex].
- [25] D. P. Barber et al. “Discovery of Three Jet Events and a Test of Quantum Chromodynamics at PETRA Energies”. In: *Phys. Rev. Lett.* 43 (1979), page 830. DOI: 10.1103/PhysRevLett.43.830.
- [26] S. Schael et al. “Precision electroweak measurements on the Z resonance”. In: *Phys. Rept.* 427 (2006), pages 257–454. DOI: 10.1016/j.physrep.2005.12.006. arXiv: hep-ex/0509008 [hep-ex].
- [27] Sabine Riemann. “Precision electroweak physics at high energies”. In: *Rept. Prog. Phys.* 73 (2010), page 126201. DOI: 10.1088/0034-4885/73/12/126201.
- [28] Kenji Abe et al. “A High precision measurement of the left-right Z boson cross-section asymmetry”. In: *Phys. Rev. Lett.* 84 (2000), pages 5945–5949. DOI: 10.1103/PhysRevLett.84.5945. arXiv: hep-ex/0004026 [hep-ex].
- [29] Koya Abe et al. “First direct measurement of the parity violating coupling of the Z_0 to the s quark”. In: *Phys. Rev. Lett.* 85 (2000), pages 5059–5063. DOI: 10.1103/PhysRevLett.85.5059. arXiv: hep-ex/0006019 [hep-ex].
- [30] Koya Abe et al. “An Improved direct measurement of leptonic coupling asymmetries with polarized Z bosons”. In: *Phys. Rev. Lett.* 86 (2001), pages 1162–1166. DOI: 10.1103/PhysRevLett.86.1162. arXiv: hep-ex/0010015 [hep-ex].

- [31] K. Abe et al. “First measurement of the left-right charge asymmetry in hadronic Z boson decays and a new determination of $\sin^{**2} \theta(W)(\text{eff})$ ”. In: *Phys. Rev. Lett.* 78 (1997), pages 17–21. DOI: 10.1103/PhysRevLett.78.17. arXiv: hep-ex/9609019 [hep-ex].
- [32] Timo Antero Aaltonen et al. “Combination of CDF and D0 W-Boson Mass Measurements”. In: *Phys. Rev.* D88.5 (2013), page 052018. DOI: 10.1103/PhysRevD.88.052018. arXiv: 1307.7627 [hep-ex].
- [33] “Combination of CDF and D0 Results on the Width of the W boson”. In: (2010). arXiv: 1003.2826 [hep-ex].
- [34] Morad Aaboud et al. “Measurement of the W-boson mass in pp collisions at $\sqrt{s} = 7$ TeV with the ATLAS detector”. In: *Eur. Phys. J.* C78.2 (2018), page 110. DOI: 10.1140/epjc/s10052-017-5475-4. arXiv: 1701.07240 [hep-ex].
- [35] ATLAS. URL: cds.cern.ch/record/2285809/files/ATLAS-CONF-2017-071.pdf.
- [36] CMS. URL: cds.cern.ch/record/2235162/files/TOP-15-012-pas.pdf.
- [37] CMS. URL: cds.cern.ch/record/2284594/files/TOP-17-007-pas.pdf.
- [38] NA62 collaboration. URL: <https://indico.cern.ch/event/714178/>.
- [39] Cari Cesarotti et al. “Interpreting the Electron EDM Constraint”. In: (2018). arXiv: 1810.07736 [hep-ph].
- [40] M. G. Aartsen et al. “Measurement of the multi-TeV neutrino cross section with IceCube using Earth absorption”. In: *Nature* 551 (2017), pages 596–600. DOI: 10.1038/nature24459. arXiv: 1711.08119 [hep-ex].
- [41] Andrea Castro. “Recent Top Quark Mass Measurements from CMS”. In: *Proceedings, 10th International Workshop on Top Quark Physics (TOP2017): Braga, Portugal, September 17-22, 2017*. 2017. arXiv: 1712.01027 [hep-ex].
- [42] PDG. URL: <http://pdg.lbl.gov/2018/reviews/rpp2018-rev-standard-model.pdf>.
- [43] P. A. R. Ade et al. “Planck 2015 results. XIII. Cosmological parameters”. In: *Astron. Astrophys.* 594 (2016), A13. DOI: 10.1051/0004-6361/201525830. arXiv: 1502.01589 [astro-ph.CO].
- [44] Evgige Corbelli and Paolo Salucci. “The Extended Rotation Curve and the Dark Matter Halo of M33”. In: *Mon. Not. Roy. Astron. Soc.* 311 (2000), pages 441–447. DOI: 10.1046/j.1365-8711.2000.03075.x. arXiv: astro-ph/9909252 [astro-ph].
- [45] S. M. Faber and R. E. Jackson. “Velocity dispersions and mass to light ratios for elliptical galaxies”. In: *Astrophys. J.* 204 (1976), page 668. DOI: 10.1086/154215.
- [46] Steven W. Allen, August E. Evrard, and Adam B. Mantz. “Cosmological Parameters from Observations of Galaxy Clusters”. In: *Ann. Rev. Astron. Astrophys.* 49 (2011), pages 409–470. DOI: 10.1146/annurev-astro-081710-102514. arXiv: 1103.4829 [astro-ph.CO].
- [47] Priyamvada Natarajan et al. “Mapping substructure in the HST Frontier Fields cluster lenses and in cosmological simulations”. In: *Mon. Not. Roy. Astron. Soc.* 468.2 (2017), pages 1962–1980. DOI: 10.1093/mnras/stw3385. arXiv: 1702.04348 [astro-ph.GA].
- [48] John F. Donoghue. “The effective field theory treatment of quantum gravity”. In: *AIP Conf. Proc.* 1483 (2012), pages 73–94. DOI: 10.1063/1.4756964. arXiv: 1209.3511 [gr-qc].
- [49] C. D. McCoy. “Does inflation solve the hot big bang model’s fine-tuning problems?” In: *Stud. Hist. Phil. Sci.* B51 (2015), pages 23–36. DOI: 10.1016/j.shpsb.2015.06.002.
- [50] R. D. Peccei. “The Strong CP problem and axions”. In: *Lect. Notes Phys.* 741 (2008). [,3(2006)], pages 3–17. DOI: 10.1007/978-3-540-73518-2_1. arXiv: hep-ph/0607268 [hep-ph].

- [51] C. Amsler et al. “Review of Particle Physics”. In: *Physics Letters B* 667.1 (2008). Review of Particle Physics, pages 1–6. ISSN: 0370-2693. DOI: <https://doi.org/10.1016/j.physletb.2008.07.018>. URL: <http://www.sciencedirect.com/science/article/pii/S0370269308008435>.
- [52] Georges Aad et al. “Combined Measurement of the Higgs Boson Mass in pp Collisions at $\sqrt{s} = 7$ and 8 TeV with the ATLAS and CMS Experiments”. In: *Phys. Rev. Lett.* 114 (2015), page 191803. DOI: 10.1103/PhysRevLett.114.191803. arXiv: 1503.07589 [hep-ex].
- [53] Susanne Mertens. “Direct Neutrino Mass Experiments”. In: *J. Phys. Conf. Ser.* 718.2 (2016), page 022013. DOI: 10.1088/1742-6596/718/2/022013. arXiv: 1605.01579 [nucl-ex].
- [54] Ivan Esteban et al. “Updated fit to three neutrino mixing: exploring the accelerator-reactor complementarity”. In: *JHEP* 01 (2017), page 087. DOI: 10.1007/JHEP01(2017)087. arXiv: 1611.01514 [hep-ph].
- [55] NuFIT. URL: <http://www.nu-fit.org/?q=node/177>.
- [56] nobel2004. URL: <https://www.nobelprize.org/prizes/physics/2004/popular-information/>.
- [57] Xiao-Gang He, Girish C. Joshi, and B. H. McKellar. “The Quantization of the Electric Charge in Gauge Theories”. In: *Europhys. Lett.* 10 (1989), page 709. DOI: 10.1209/0295-5075/10/8/002.
- [58] Stefano Bertolini, Luca Di Luzio, and Michal Malinsky. “Intermediate mass scales in the non-supersymmetric SO(10) grand unification: A Reappraisal”. In: *Phys. Rev.* D80 (2009), page 015013. DOI: 10.1103/PhysRevD.80.015013. arXiv: 0903.4049 [hep-ph].
- [59] Hong-Wei Yu. “SU(8) GUT MODELS WITH STABLE PROTON, N ANTI-N OSCILLATIONS, FRACTIONAL CHARGES AND LOW MASS MONOPOLES”. In: *Phys. Lett.* 142B (1984), pages 42–46. DOI: 10.1016/0370-2693(84)91132-8.
- [60] Xiao-Gang Wen and Edward Witten. “Electric and Magnetic Charges in Superstring Models”. In: *Nucl. Phys.* B261 (1985), pages 651–677. DOI: 10.1016/0550-3213(85)90592-9.
- [61] Gregory G. Athanasiou et al. “Remarks on Wilson Lines, Modular Invariance and Possible String Relics in Calabi-yau Compactifications”. In: *Phys. Lett.* B214 (1988), pages 55–62. DOI: 10.1016/0370-2693(88)90451-0.
- [62] Stephen M. Barr, D. B. Reiss, and A. Zee. “Fractional Charges, Monopoles and Peculiar Photons”. In: *Phys. Rev. Lett.* 50 (1983), page 317. DOI: 10.1103/PhysRevLett.50.317.
- [63] P. H. Frampton and T. W. Kephart. “Fractionally Charged Particles as Evidence for Supersymmetry”. In: *Phys. Rev. Lett.* 49 (1982), page 1310. DOI: 10.1103/PhysRevLett.49.1310.
- [64] Katsuji Yamamoto. “Fractionally Charged Leptons in the SO(14) GUT”. In: *Phys. Lett.* 120B (1983), pages 157–160. DOI: 10.1016/0370-2693(83)90643-3.
- [65] Fang-xiao Dong et al. “Fractional Charges, Monopoles and Peculiar Photons in SO(18) GUT Models”. In: *Phys. Lett.* 129B (1983), pages 405–410. DOI: 10.1016/0370-2693(83)90129-6.
- [66] Xiang-Dong Jiang and Xian-Jian Zhou. “SO(10) X SO(8) MODEL WITH FRACTIONAL CHARGES, MONOPOLES AND PECULIAR PHOTONS. (IN CHINESE)”. In: *HEPNP* 9 (1985), pages 421–429.
- [67] K. Abe et al. “Search for proton decay via $p \rightarrow e^+\pi^0$ and $p \rightarrow \mu^+\pi^0$ in 0.31 megaton years exposure of the Super-Kamiokande water Cherenkov detector”. In: *Phys. Rev.* D95.1 (2017), page 012004. DOI: 10.1103/PhysRevD.95.012004. arXiv: 1610.03597 [hep-ex].

- [68] Ignatios Antoniadis and K. Benakli. “Fractionally charged particles and supersymmetry breaking in 4-D strings”. In: *Phys. Lett.* B295 (1992). [Erratum: *Phys. Lett.* B407,449(1997)], pages 219–224. DOI: 10.1016/S0370-2693(97)00755-7, 10.1016/0370-2693(92)91557-P. arXiv: hep-th/9209020 [hep-th].
- [69] Bob Holdom. “Two U(1)’s and Epsilon Charge Shifts”. In: *Phys. Lett.* 166B (1986), pages 196–198. DOI: 10.1016/0370-2693(86)91377-8.
- [70] Eder Izaguirre and Itay Yavin. “New window to millicharged particles at the LHC”. In: *Phys. Rev.* D92.3 (2015), page 035014. DOI: 10.1103/PhysRevD.92.035014. arXiv: 1506.04760 [hep-ph].
- [71] David E. Brahm and Lawrence J. Hall. “U(1)-prime DARK MATTER”. In: *Phys. Rev.* D41 (1990), page 1067. DOI: 10.1103/PhysRevD.41.1067.
- [72] C. Boehm and Pierre Fayet. “Scalar dark matter candidates”. In: *Nucl. Phys.* B683 (2004), pages 219–263. DOI: 10.1016/j.nuclphysb.2004.01.015. arXiv: hep-ph/0305261 [hep-ph].
- [73] Maxim Pospelov, Adam Ritz, and Mikhail B. Voloshin. “Secluded WIMP Dark Matter”. In: *Phys. Lett.* B662 (2008), pages 53–61. DOI: 10.1016/j.physletb.2008.02.052. arXiv: 0711.4866 [hep-ph].
- [74] James D. Bjorken et al. “New Fixed-Target Experiments to Search for Dark Gauge Forces”. In: *Phys. Rev.* D80 (2009), page 075018. DOI: 10.1103/PhysRevD.80.075018. arXiv: 0906.0580 [hep-ph].
- [75] Gabriel Magill et al. “Millicharged particles in neutrino experiments”. In: (2018). arXiv: 1806.03310 [hep-ph].
- [76] R. Acciarri et al. “Long-Baseline Neutrino Facility (LBNF) and Deep Underground Neutrino Experiment (DUNE)”. In: (2015). arXiv: 1512.06148 [physics.ins-det].
- [77] M. Anelli et al. “A facility to Search for Hidden Particles (SHiP) at the CERN SPS”. In: (2015). arXiv: 1504.04956 [physics.ins-det].
- [78] Marco Battaglieri et al. “US Cosmic Visions: New Ideas in Dark Matter 2017: Community Report”. In: (2017). arXiv: 1707.04591 [hep-ph].
- [79] S. I. Alvis et al. “First Limit on the Direct Detection of Lightly Ionizing Particles for Electric Charge as Low as e/1000 with the Majorana Demonstrator”. In: *Phys. Rev. Lett.* 120.21 (2018), page 211804. DOI: 10.1103/PhysRevLett.120.211804. arXiv: 1801.10145 [hep-ex].
- [80] L. Lyons. “Quark Search Experiments at Accelerators and in Cosmic Rays”. In: *Phys. Rept.* 129 (1985), page 225. DOI: 10.1016/0370-1573(85)90011-0.
- [81] J. J. Aubert et al. “A Search for Free Quarks in Deep Inelastic Muon Scattering”. In: *Phys. Lett.* 133B (1983), page 461. DOI: 10.1016/0370-2693(83)90828-6.
- [82] A. E. Bondar et al. “SEARCH FOR LIGHT PARTICLES WITH CHARGE 2/3 IN e+ e- ANNIHILATION”. In: *JETP Lett.* 40 (1984). [*Pisma Zh. Eksp. Teor. Fiz.* 40,440(1984)], pages 1265–1268.
- [83] H. Aihara et al. “Search for $q = 2/3e$ and $q = 1/3e$ particles produced in e^+e^- annihilations”. In: *Phys. Rev. Lett.* 52 (1984), page 2332. DOI: 10.1103/PhysRevLett.52.2332.
- [84] G. Abbiendi et al. “Search for stable and longlived massive charged particles in e+ e- collisions at $s^{**}(1/2) = 130\text{-GeV}$ to 209-GeV ”. In: *Phys. Lett.* B572 (2003), pages 8–20. DOI: 10.1016/S0370-2693(03)00639-7. arXiv: hep-ex/0305031 [hep-ex].
- [85] P. Abreu et al. “Search for stable heavy charged particles in e+ e- collisions at $s^{**}(1/2) = 130\text{-GeV}$ to 136-GeV , 161-GeV and 172-GeV ”. In: *Phys. Lett.* B396 (1997), pages 315–326. DOI: 10.1016/S0370-2693(97)00152-4.

- [86] R. Akers et al. “Search for heavy charged particles and for particles with anomalous charge in e^+e^- collisions at LEP”. In: *Z. Phys.* C67 (1995), pages 203–212. DOI: 10.1007/BF01571281.
- [87] D. Buskulic et al. “Search for particles with unexpected mass and charge in Z decays”. In: *Phys. Lett.* B303 (1993), pages 198–208. DOI: 10.1016/0370-2693(93)90066-Q.
- [88] M. Banner et al. “A New Search for Relativistic Particles With Fractional Electric Charge at the CERN $p\bar{p}$ Collider”. In: *Phys. Lett.* 156B (1985), pages 129–133. DOI: 10.1016/0370-2693(85)91368-1.
- [89] F. Abe et al. “Limits on the production of massive stable charged particles”. In: *Phys. Rev.* D46 (1992), R1889–R1894. DOI: 10.1103/PhysRevD.46.R1889.
- [90] D. Acosta et al. “Search for long-lived charged massive particles in $\bar{p}p$ collisions at $\sqrt{s} = 1.8$ TeV”. In: *Phys. Rev. Lett.* 90 (2003), page 131801. DOI: 10.1103/PhysRevLett.90.131801. arXiv: hep-ex/0211064 [hep-ex].
- [91] Serguei Chatrchyan et al. “Search for fractionally charged particles in pp collisions at $\sqrt{s} = 7$ TeV”. In: *Phys. Rev.* D87.9 (2013), page 092008. DOI: 10.1103/PhysRevD.87.092008. arXiv: 1210.2311 [hep-ex].
- [92] M. Ambrosio et al. “Final search for lightly ionizing particles with the MACRO detector”. In: (2004). arXiv: hep-ex/0402006 [hep-ex].
- [93] M. Mori et al. “Search for fractionally charged particles in Kamiokande-II”. In: *Phys. Rev.* D43 (1991), pages 2843–2846. DOI: 10.1103/PhysRevD.43.2843.
- [94] G. Giacomelli and A. Margiotta. “The MACRO Experiment at Gran Sasso”. In: *Charles Peck Fest Pasadena, California, January 21, 2005*. 2007. arXiv: 0707.1691 [hep-ex].
- [95] Thomas K. Gaisser, Ralph Engel, and Elisa Resconi. *Cosmic Rays and Particle Physics*. Cambridge University Press, 2016. ISBN: 9780521016469, 9781316598917. URL: <http://www.cambridge.org/de/academic/subjects/physics/cosmology-relativity-and-gravitation/cosmic-rays-and-particle-physics-2nd-edition?format=HB>.
- [96] The Nobel Prize. URL: <https://www.nobelprize.org/prizes/physics/1936/ceremony-speech/>.
- [97] J. Clay. *Penetrating radiation*. Volume 30. 1927, pages 1115–1127.
- [98] R. A. Millikan and G. H. Cameron. “The Origin of the Cosmic Rays”. In: *Phys. Rev.* 32 (4 Oct. 1928), pages 533–557. DOI: 10.1103/PhysRev.32.533. URL: <https://link.aps.org/doi/10.1103/PhysRev.32.533>.
- [99] M.H. Israel et al. “Isotopic Composition of Cosmic Rays: Results from the Cosmic Ray Isotope Spectrometer on the ACE Spacecraft”. In: *Nuclear Physics A* 758 (2005). Nuclei in the Cosmos VIII, pages 201–208. ISSN: 0375-9474. DOI: <https://doi.org/10.1016/j.nuclphysa.2005.05.038>. URL: <http://www.sciencedirect.com/science/article/pii/S037594740500686X>.
- [100] Pasquale Blasi. “The Origin of Galactic Cosmic Rays”. In: *Astron. Astrophys. Rev.* 21 (2013), page 70. DOI: 10.1007/s00159-013-0070-7. arXiv: 1311.7346 [astro-ph.HE].
- [101] Thomas K. Gaisser, Todor Stanev, and Serap Tilav. “Cosmic Ray Energy Spectrum from Measurements of Air Showers”. In: *Front. Phys.(Beijing)* 8 (2013), pages 748–758. DOI: 10.1007/s11467-013-0319-7. arXiv: 1303.3565 [astro-ph.HE].
- [102] M A Malkov and L O’C Drury. “Nonlinear theory of diffusive acceleration of particles by shock waves”. In: *Reports on Progress in Physics* 64.4 (2001), page 429. URL: <http://stacks.iop.org/0034-4885/64/i=4/a=201>.
- [103] “Detection of the Small Magellanic Cloud in gamma-rays with Fermi/LAT”. In: *Astron. Astrophys.* 523 (2010), A46. DOI: 10.1051/0004-6361/201014855. arXiv: 1008.2127 [astro-ph.HE].

- [104] M. Ackermann et al. “Detection of the Characteristic Pion-Decay Signature in Supernova Remnants”. In: *Science* 339 (2013), page 807. DOI: 10.1126/science.1231160. arXiv: 1302.3307 [astro-ph.HE].
- [105] W. D. Apel et al. “Kneelike structure in the spectrum of the heavy component of cosmic rays observed with KASCADE-Grande”. In: *Phys. Rev. Lett.* 107 (2011), page 171104. DOI: 10.1103/PhysRevLett.107.171104. arXiv: 1107.5885 [astro-ph.HE].
- [106] A. P. Garyaka et al. “All-particle primary energy spectrum in the 3–200 PeV energy range”. In: *J. Phys.* G35 (2008), page 115201. DOI: 10.1088/0954-3899/35/11/115201. arXiv: 0808.1421 [astro-ph].
- [107] Kenneth Greisen. “End to the cosmic ray spectrum?” In: *Phys. Rev. Lett.* 16 (1966), pages 748–750. DOI: 10.1103/PhysRevLett.16.748.
- [108] G. T. Zatsepin and V. A. Kuzmin. “Upper limit of the spectrum of cosmic rays”. In: *JETP Lett.* 4 (1966). [Pisma Zh. Eksp. Teor. Fiz. 4, 114 (1966)], pages 78–80.
- [109] J. Bellido et al. “Proceedings of Science”. In: *ICRC* 301 (506 2017).
- [110] A. M. Hillas. “The Origin of Ultrahigh-Energy Cosmic Rays”. In: *Ann. Rev. Astron. Astrophys.* 22 (1984), pages 425–444. DOI: 10.1146/annurev.aa.22.090184.002233.
- [111] Pablo M. Bauleo and Julio Rodriguez Martino. “The dawn of the particle astronomy era in ultra-high-energy cosmic rays”. In: *Nature* 458N7240 (2009), pages 847–851. DOI: 10.1038/nature07948.
- [112] M. Nagano and Alan A. Watson. “Observations and implications of the ultrahigh-energy cosmic rays”. In: *Rev. Mod. Phys.* 72 (2000), pages 689–732. DOI: 10.1103/RevModPhys.72.689.
- [113] Alexander Aab et al. “Observation of a Large-scale Anisotropy in the Arrival Directions of Cosmic Rays above 8×10^{18} eV”. In: *Science* 357.6537 (2017), pages 1266–1270. DOI: 10.1126/science.aan4338. arXiv: 1709.07321 [astro-ph.HE].
- [114] E. Waxman. “IceCube’s Neutrinos: The beginning of extra-Galactic neutrino astrophysics?” In: *Proceedings, 9th Rencontres du Vietnam: Windows on the Universe: Quy Nhon, Vietnam, August 11–17, 2013.* 2013, pages 161–168. arXiv: 1312.0558 [astro-ph.HE].
- [115] P. O. Lagage and C. J. Cesarsky. “The maximum energy of cosmic rays accelerated by supernova shocks”. In: *Astron. Astrophys.* 125 (1983), pages 249–257.
- [116] T. Stanev. *High Energy Cosmic Rays*. Springer Praxis Books. Springer Berlin Heidelberg, 2010. ISBN: 9783540851486. URL: <https://books.google.be/books?id=1y9YEYHAfBMC>.
- [117] C. Megan Urry and Paolo Padovani. “Unified schemes for radio-loud active galactic nuclei”. In: *Publ. Astron. Soc. Pac.* 107 (1995), page 803. DOI: 10.1086/133630. arXiv: astro-ph/9506063 [astro-ph].
- [118] Robert Antonucci. “Unified models for active galactic nuclei and quasars”. In: *Ann. Rev. Astron. Astrophys.* 31 (1993), pages 473–521. DOI: 10.1146/annurev.aa.31.090193.002353.
- [119] Demosthenes Kazanas et al. “Toward a Unified AGN Structure”. In: (2012). arXiv: 1206.5022 [astro-ph.HE].
- [120] J. Abraham et al. “Correlation of the highest-energy cosmic rays with the positions of nearby active galactic nuclei”. In: *Astropart. Phys.* 29 (2008). [Erratum: Astropart. Phys. 30, 45 (2008)], pages 188–204. DOI: 10.1016/j.astropartphys.2008.06.004, 10.1016/j.astropartphys.2008.01.002. arXiv: 0712.2843 [astro-ph].
- [121] Ray W. Klebesadel, Ian B. Strong, and Roy A. Olson. “Observations of Gamma-Ray Bursts of Cosmic Origin”. In: *Astrophys. J.* 182 (1973), pages L85–L88. DOI: 10.1086/181225.
- [122] C. A. Meegan et al. “Spatial distribution of gamma-ray bursts observed by BATSE”. In: *Nature* 355 (1992), pages 143–145. DOI: 10.1038/355143a0.

- [123] B. P. Abbott et al. “GW170817: Observation of Gravitational Waves from a Binary Neutron Star Inspiral”. In: *Phys. Rev. Lett.* 119.16 (2017), page 161101. DOI: 10.1103/PhysRevLett.119.161101. arXiv: 1710.05832 [gr-qc].
- [124] B. P. Abbott et al. “GW170814: A Three-Detector Observation of Gravitational Waves from a Binary Black Hole Coalescence”. In: *Phys. Rev. Lett.* 119.14 (2017), page 141101. DOI: 10.1103/PhysRevLett.119.141101. arXiv: 1709.09660 [gr-qc].
- [125] B.. P.. Abbott et al. “GW170608: Observation of a 19-solar-mass Binary Black Hole Coalescence”. In: *Astrophys. J.* 851.2 (2017), page L35. DOI: 10.3847/2041-8213/aa9f0c. arXiv: 1711.05578 [astro-ph.HE].
- [126] Benjamin P. Abbott et al. “GW170104: Observation of a 50-Solar-Mass Binary Black Hole Coalescence at Redshift 0.2”. In: *Phys. Rev. Lett.* 118.22 (2017). [Erratum: Phys. Rev. Lett.121,no.12,129901(2018)], page 221101. DOI: 10.1103/PhysRevLett.118.221101, 10.1103/PhysRevLett.121.129901. arXiv: 1706.01812 [gr-qc].
- [127] B. P. Abbott et al. “GW151226: Observation of Gravitational Waves from a 22-Solar-Mass Binary Black Hole Coalescence”. In: *Phys. Rev. Lett.* 116.24 (2016), page 241103. DOI: 10.1103/PhysRevLett.116.241103. arXiv: 1606.04855 [gr-qc].
- [128] F. Acero. “Detection of Gamma Rays From a Starburst Galaxy”. In: *Science* 326 (2009), page 1080. DOI: 10.1126/science.1178826. arXiv: 0909.4651 [astro-ph.HE].
- [129] Niklas Karlsson. “Discovery of VHE Gamma-ray Emission from the Starburst Galaxy M82”. In: (2009). arXiv: 0912.3807 [astro-ph.HE].
- [130] Kohta Murase, Susumu Inoue, and Shigehiro Nagataki. “Cosmic Rays above the Second Knee from Clusters of Galaxies and Associated High-Energy Neutrino Emission”. In: *The Astrophysical Journal Letters* 689.2 (2008), page L105. URL: <http://stacks.iop.org/1538-4357/689/i=2/a=L105>.
- [131] C. Grupen. *Astroparticle physics*. 2005. ISBN: 9783540253129. URL: <http://www.springer.com/book/3-540-25312-2>.
- [132] U. F. Katz and Ch. Spiering. “High-Energy Neutrino Astrophysics: Status and Perspectives”. In: *Prog. Part. Nucl. Phys.* 67 (2012), pages 651–704. DOI: 10.1016/j.ppnp.2011.12.001. arXiv: 1111.0507 [astro-ph.HE].
- [133] Morihiro Honda et al. “Calculation of atmospheric neutrino flux using the interaction model calibrated with atmospheric muon data”. In: *Phys. Rev. D* 75 (2007), page 043006. DOI: 10.1103/PhysRevD.75.043006. arXiv: astro-ph/0611418 [astro-ph].
- [134] M. G. Aartsen et al. “The IceCube Neutrino Observatory - Contributions to ICRC 2017 Part II: Properties of the Atmospheric and Astrophysical Neutrino Flux”. In: (2017). arXiv: 1710.01191 [astro-ph.HE].
- [135] Kiyoshi Niu, Eiko Mikumo, and Yasuko Maeda. “A Possible Decay in Flight of a New Type Particle”. In: *Progress of Theoretical Physics* 46.5 (1971), pages 1644–1646. DOI: 10.1143/PTP.46.1644. eprint: /oup/backfile/content_public/journal/ptp/46/5/10.1143/ptp.46.1644/2/46-5-1644.pdf. URL: <http://dx.doi.org/10.1143/PTP.46.1644>.
- [136] Rikard Enberg, Mary Hall Reno, and Ina Sarcevic. “Prompt neutrino fluxes from atmospheric charm”. In: *Phys. Rev. D* 78 (2008), page 043005. DOI: 10.1103/PhysRevD.78.043005. arXiv: 0806.0418 [hep-ph].
- [137] M. G. Aartsen et al. “Multimessenger observations of a flaring blazar coincident with high-energy neutrino IceCube-170922A”. In: *Science* 361.6398 (2018), eaat1378. DOI: 10.1126/science.aat1378. arXiv: 1807.08816 [astro-ph.HE].
- [138] Kate Scholberg. “Supernova Neutrino Detection”. In: *Ann. Rev. Nucl. Part. Sci.* 62 (2012), pages 81–103. DOI: 10.1146/annurev-nucl-102711-095006. arXiv: 1205.6003 [astro-ph.IM].

- [139] Lutz Kopke. “Supernova Neutrino Detection with IceCube”. In: *J. Phys. Conf. Ser.* 309 (2011), page 012029. DOI: 10.1088/1742-6596/309/1/012029. arXiv: 1106.6225 [astro-ph.HE].
- [140] Aya Ishihara. “Diffuse Neutrino Fluxes and GZK Neutrinos with IceCube”. In: *JPS Conf. Proc.* 15 (2017), page 011008. DOI: 10.7566/JPSCP.15.011008.
- [141] nobel1958. URL: <https://www.nobelprize.org/prizes/physics/1958/summary/>.
- [142] “Design, Implementation and Test of a New Feature Extractor for the IceCube Neutrino Observatory”. In: (2010).
- [143] Paul H. Barrett et al. “Interpretation of Cosmic-Ray Measurements Far Underground”. In: *Rev. Mod. Phys.* 24.3 (1952), pages 133–178. DOI: 10.1103/RevModPhys.24.133.
- [144] Dmitry Chirkin and Wolfgang Rhode. “Muon Monte Carlo: A High-precision tool for muon propagation through matter”. In: (2004). arXiv: hep-ph/0407075 [hep-ph].
- [145] Dmitry Chirkin. “Study of South Pole ice transparency with IceCube flashers”. In: *Proceedings, 32nd International Cosmic Ray Conference (ICRC 2011): Beijing, China, August 11-18, 2011*. Volume 4, page 161. DOI: 10.7529/ICRC2011/V04/0333.
- [146] S. R. Kelner, R. P. Kokoulin, and A. A. Petrukhin. “About cross-section for high-energy muon bremsstrahlung”. In: (1995).
- [147] AMANDA collaboration. URL: <http://amanda.uci.edu/> (cited on page 3).
- [148] E. Andres et al. “The AMANDA neutrino telescope: Principle of operation and first results”. In: *Astropart. Phys.* 13 (2000), pages 1–20. DOI: 10.1016/S0927-6505(99)00092-4. arXiv: astro-ph/9906203 [astro-ph] (cited on page 3).
- [149] J. Ahrens et al. “Observation of high-energy atmospheric neutrinos with the Antarctic Muon and Neutrino Detector Array”. In: *Phys. Rev.* D66 (2002), page 012005. DOI: 10.1103/PhysRevD.66.012005. arXiv: astro-ph/0205109 [astro-ph] (cited on page 3).
- [150] R. Abbasi et al. “The Design and Performance of IceCube DeepCore”. In: *Astropart. Phys.* 35 (2012), pages 615–624. DOI: 10.1016/j.astropartphys.2012.01.004. arXiv: 1109.6096 [astro-ph.IM] (cited on page 5).
- [151] Nicholas Choma et al. “Graph Neural Networks for IceCube Signal Classification”. In: (2018). arXiv: 1809.06166 [cs.LG] (cited on page 6).
- [152] M. G. Aartsen et al. “The IceCube Neutrino Observatory: Instrumentation and Online Systems”. In: *JINST* 12.03 (2017), P03012. DOI: 10.1088/1748-0221/12/03/P03012. arXiv: 1612.05093 [astro-ph.IM] (cited on pages 7, 9, 10).
- [153] R. Abbasi et al. “Calibration and Characterization of the IceCube Photomultiplier Tube”. In: *Nucl. Instrum. Meth.* A618 (2010), pages 139–152. DOI: 10.1016/j.nima.2010.03.102. arXiv: 1002.2442 [astro-ph.IM] (cited on page 7).
- [154] M. G. Aartsen et al. “Measurement of South Pole ice transparency with the IceCube LED calibration system”. In: *Nucl. Instrum. Meth.* A711 (2013), pages 73–89. DOI: 10.1016/j.nima.2013.01.054. arXiv: 1301.5361 [astro-ph.IM] (cited on pages 8, 14).
- [155] M. G. Aartsen et al. “The IceCube Realtime Alert System”. In: *Astropart. Phys.* 92 (2017), pages 30–41. DOI: 10.1016/j.astropartphys.2017.05.002. arXiv: 1612.06028 [astro-ph.HE] (cited on page 13).
- [156] Dariusz Góra. “High-Energy Gamma-Ray Follow-Up Program Using Neutrino Triggers from IceCube”. In: *Proceedings, 33rd International Cosmic Ray Conference (ICRC2013): Rio de Janeiro, Brazil, July 2-9, 2013*, page 0537. URL: <http://www.cbpf.br/%7Eicrc2013/papers/icrc2013-0537.pdf> (cited on page 13).
- [157] The IceCube collaboration. URL: https://wiki.icecube.wisc.edu/index.php/Pass2_Re-Processing (cited on page 14).

- [158] M. Ackermann et al. “Optical properties of deep glacial ice at the South Pole”. In: *J. Geophys. Res. Atmos.* 111.D13 (2006), page D13203. DOI: 10.1029/2005JD006687 (cited on page 14).
- [159] Dmitry Chirkin. “Evidence of optical anisotropy of the South Pole ice”. In: *Proceedings, 33rd International Cosmic Ray Conference (ICRC2013): Rio de Janeiro, Brazil, July 2-9, 2013*, page 0580. URL: <http://www.cbpf.br/%7Eicrc2013/papers/icrc2013-0580.pdf> (cited on page 15).
- [160] The IceCube Collaboration. URL: https://docushare.icecube.wisc.edu/dsweb/Get/Document-56552/dst_proposal_2011.pdf (cited on page 16).
- [161] M. G. Aartsen et al. “Search for steady point-like sources in the astrophysical muon neutrino flux with 8 years of IceCube data”. In: (2018). arXiv: 1811.07979 [hep-ph] (cited on page 16).
- [162] The IceCube Collaboration. URL: https://icecube.wisc.edu/~kjero/Bootcamp/2015/Notebooks/Reconstruction_Introduction.html (cited on page 17).
- [163] Samridha Kunwar et al. “The IceTop Scintillator Upgrade”. In: *PoS ICRC2017* (2018), page 401. DOI: 10.22323/1.301.0401 (cited on page 16).
- [164] Jan Auffenberg. “IceAct: Imaging Air Cherenkov Telescopes with SiPMs at the South Pole for IceCube-Gen2”. In: *PoS ICRC2017* (2018), page 1055. DOI: 10.22323/1.301.1055 (cited on page 16).
- [165] Satoshi Shimizu et al. “Overview and performance of the D-Egg optical sensor for IceCube-Gen2”. In: *PoS ICRC2017* (2018), page 1051. DOI: 10.22323/1.301.1051 (cited on page 17).
- [166] Lew Classen et al. “The mDOM - A multi-PMT digital optical module for the IceCube-Gen2 neutrino telescope”. In: *PoS ICRC2017* (2018), page 1047. DOI: 10.22323/1.301.1047 (cited on page 17).
- [167] M. Jeong and W. Kang. “A camera system for IceCube-Gen2”. In: *PoS ICRC2017* (2018), page 1040. DOI: 10.22323/1.301.1040 (cited on page 17).
- [168] Elisa Resconi, Kai Krings, and Kai Krings Martin Rongen. “The Precision Optical CALibration Module for IceCube-Gen2: First Prototype”. In: *PoS ICRC2017* (2018), page 934. DOI: 10.22323/1.301.0934 (cited on page 17).
- [169] Erik Blaufuss, C. Kopper, and C. Haack. “The IceCube-Gen2 High Energy Array”. In: *PoS ICRC2015* (2016), page 1146. DOI: 10.22323/1.236.1146 (cited on page 18).
- [170] Markus Ahlers and Francis Halzen. “Pinpointing Extragalactic Neutrino Sources in Light of Recent IceCube Observations”. In: *Phys. Rev. D* 90.4 (2014), page 043005. DOI: 10.1103/PhysRevD.90.043005. arXiv: 1406.2160 [astro-ph.HE] (cited on page 18).
- [171] Sebastian Euler, Javier Gonzalez, and Ben Roberts. “Simulation Studies for a Surface Veto Array to Identify Astrophysical Neutrinos at the South Pole”. In: *PoS ICRC2015* (2016), page 1070. DOI: 10.22323/1.236.1070 (cited on page 19).
- [172] Frank G. Schröder. “Radio detection of Cosmic-Ray Air Showers and High-Energy Neutrinos”. In: *Prog. Part. Nucl. Phys.* 93 (2017), pages 1–68. DOI: 10.1016/j.ppnp.2016.12.002. arXiv: 1607.08781 [astro-ph.IM] (cited on page 19).
- [173] P. Allison et al. “Performance of two Askaryan Radio Array stations and first results in the search for ultrahigh energy neutrinos”. In: *Phys. Rev. D* 93.8 (2016), page 082003. DOI: 10.1103/PhysRevD.93.082003. arXiv: 1507.08991 [astro-ph.HE] (cited on page 19).
- [174] Christian Glaser. “ARIANNA: Measurement of cosmic rays with a radio neutrino detector in Antarctica”. In: *Acoustic and Radio EeV Neutrino Detection Activities (ARENA 2018) Catania, Italy, June 12-15, 2018*. 2018. arXiv: 1811.10661 [astro-ph.IM] (cited on page 19).

- [175] Don Colladay and V. Alan Kostelecky. “Lorentz violating extension of the standard model”. In: *Phys. Rev.* D58 (1998), page 116002. DOI: 10.1103/PhysRevD.58.116002. arXiv: hep-ph/9809521 [hep-ph] (cited on page 20).
- [176] M. G. Aartsen et al. “Neutrino Interferometry for High-Precision Tests of Lorentz Symmetry with IceCube”. In: *Nature Phys.* 14.9 (2018), pages 961–966. DOI: 10.1038/s41567-018-0172-2. arXiv: 1709.03434 [hep-ex] (cited on page 20).
- [177] R. Abbasi et al. “Search for a Lorentz-violating sidereal signal with atmospheric neutrinos in IceCube”. In: *Phys. Rev.* D82 (2010), page 112003. DOI: 10.1103/PhysRevD.82.112003. arXiv: 1010.4096 [astro-ph.HE] (cited on page 20).
- [178] M. G. Aartsen et al. “Search for Neutrinos from Dark Matter Self-Annihilations in the center of the Milky Way with 3 years of IceCube/DeepCore”. In: *Eur. Phys. J.* C77.9 (2017), page 627. DOI: 10.1140/epjc/s10052-017-5213-y. arXiv: 1705.08103 [hep-ex] (cited on page 21).
- [179] M. G. Aartsen et al. “Search for annihilating dark matter in the Sun with 3 years of IceCube data”. In: *Eur. Phys. J.* C77.3 (2017), page 146. DOI: 10.1140/epjc/s10052-017-4689-9. arXiv: 1612.05949 [astro-ph.HE] (cited on page 21).
- [180] R. Abbasi et al. “Limits on a muon flux from Kaluza-Klein dark matter annihilations in the Sun from the IceCube 22-string detector”. In: *Phys. Rev.* D81 (2010), page 057101. DOI: 10.1103/PhysRevD.81.057101. arXiv: 0910.4480 [astro-ph.CO] (cited on page 21).
- [181] M. G. Aartsen et al. “First search for dark matter annihilations in the Earth with the IceCube Detector”. In: *Eur. Phys. J.* C77.2 (2017), page 82. DOI: 10.1140/epjc/s10052-016-4582-y. arXiv: 1609.01492 [astro-ph.HE] (cited on page 21).
- [182] “Quantised singularities in the electromagnetic field,” in: *Proceedings of the Royal Society of London A: Mathematical, Physical and Engineering Sciences* 133.821 (1931), pages 60–72. ISSN: 0950-1207. DOI: 10.1098/rspa.1931.0130. eprint: <http://rspa.royalsocietypublishing.org/content/133/821/60.full.pdf>. URL: <http://rspa.royalsocietypublishing.org/content/133/821/60> (cited on page 21).
- [183] G.’t Hooft. “Magnetic monopoles in unified gauge theories”. In: *Nuclear Physics B* 79.2 (1974), pages 276–284. ISSN: 0550-3213. DOI: [https://doi.org/10.1016/0550-3213\(74\)90486-6](https://doi.org/10.1016/0550-3213(74)90486-6). URL: <http://www.sciencedirect.com/science/article/pii/0550321374904866> (cited on page 21).
- [184] Alexander M. Polyakov. “Particle Spectrum in the Quantum Field Theory”. In: *JETP Lett.* 20 (1974). [,300(1974)], pages 194–195 (cited on page 21).
- [185] M. G. Aartsen et al. “Search for non-relativistic Magnetic Monopoles with IceCube”. In: *Eur. Phys. J.* C74.7 (2014), page 2938. DOI: 10.1140/epjc/s10052-014-2938-8. arXiv: 1402.3460 [astro-ph.CO] (cited on page 22).
- [186] D Schultz. “IceProd 2: A Next Generation Data Analysis Framework for the IceCube Neutrino Observatory”. In: *Journal of Physics: Conference Series* 664.6 (2015), page 062056. URL: <http://stacks.iop.org/1742-6596/664/i=6/a=062056>.
- [187] Ralph Engel et al. “Towards the next generation of CORSIKA: A framework for the simulation of particle cascades in astroparticle physics”. In: (2018). arXiv: 1808.08226 [astro-ph.IM].
- [188] Giuseppe Battistoni et al. “Overview of the FLUKA code”. In: *Annals Nucl. Energy* 82 (2015), pages 10–18. DOI: 10.1016/j.anucene.2014.11.007.
- [189] Askhat Gazizov and Marek P. Kowalski. “ANIS: High energy neutrino generator for neutrino telescopes”. In: *Comput. Phys. Commun.* 172 (2005), pages 203–213. DOI: 10.1016/j.cpc.2005.03.113. arXiv: astro-ph/0406439 [astro-ph].
- [190] M. G. Aartsen et al. “Observation of High-Energy Astrophysical Neutrinos in Three Years of IceCube Data”. In: *Phys. Rev. Lett.* 113 (2014), page 101101. DOI: 10.1103/PhysRevLett.113.101101. arXiv: 1405.5303 [astro-ph.HE].

- [191] C. Andreopoulos et al. “The GENIE Neutrino Monte Carlo Generator”. In: *Nucl. Instrum. Meth.* A614 (2010), pages 87–104. DOI: 10.1016/j.nima.2009.12.009. arXiv: 0905.2517 [hep-ph].
- [192] Costas Andreopoulos et al. “The GENIE Neutrino Monte Carlo Generator: Physics and User Manual”. In: (2015). arXiv: 1510.05494 [hep-ph].
- [193] M. Honda et al. “Atmospheric neutrino flux calculation using the NRLMSISE-00 atmospheric model”. In: *Phys. Rev.* D92.2 (2015), page 023004. DOI: 10.1103/PhysRevD.92.023004. arXiv: 1502.03916 [astro-ph.HE].
- [194] Joerg R. Hoerandel. “On the knee in the energy spectrum of cosmic rays”. In: *Astropart. Phys.* 19 (2003), pages 193–220. DOI: 10.1016/S0927-6505(02)00198-6. arXiv: astro-ph/0210453 [astro-ph].
- [195] Thomas K. Gaisser. “Spectrum of cosmic-ray nucleons, kaon production, and the atmospheric muon charge ratio”. In: *Astropart. Phys.* 35 (2012), pages 801–806. DOI: 10.1016/j.astropartphys.2012.02.010. arXiv: 1111.6675 [astro-ph.HE].
- [196] G. D. Barr et al. “Three-dimensional calculation of atmospheric neutrinos”. In: *Phys. Rev. D* 70 (2 July 2004), page 023006. DOI: 10.1103/PhysRevD.70.023006. URL: <https://link.aps.org/doi/10.1103/PhysRevD.70.023006>.
- [197] Mario Dunsch et al. “Recent Improvements for the Lepton Propagator PROPOSAL”. In: (2018). arXiv: 1809.07740 [hep-ph].
- [198] Johan Lundberg et al. “Light tracking for glaciers and oceans: Scattering and absorption in heterogeneous media with Photonics”. In: *Nucl. Instrum. Meth.* A581 (2007), pages 619–631. DOI: 10.1016/j.nima.2007.07.143. arXiv: astro-ph/0702108 [ASTRO-PH].
- [199] K. J. Ma et al. “Time and Amplitude of Afterpulse Measured with a Large Size Photomultiplier Tube”. In: *Nucl. Instrum. Meth.* A629 (2011), pages 93–100. DOI: 10.1016/j.nima.2010.11.095. arXiv: 0911.5336 [physics.ins-det].
- [200] J. Ahrens et al. “Muon track reconstruction and data selection techniques in AMANDA”. In: *Nucl. Instrum. Meth.* A524 (2004), pages 169–194. DOI: 10.1016/j.nima.2004.01.065. arXiv: astro-ph/0407044 [astro-ph].
- [201] M. G. Aartsen et al. “Improvement in Fast Particle Track Reconstruction with Robust Statistics”. In: *Nucl. Instrum. Meth.* A736 (2014), pages 143–149. DOI: 10.1016/j.nima.2013.10.074. arXiv: 1308.5501 [astro-ph.IM].
- [202] IceCube collaboration. URL: https://internal-apps.icecube.wisc.edu/reports/data/icecube/2014/04/001/icecube_201404001_v1.pdf.
- [203] Stef Verpoest. URL: https://lib.ugent.be/fulltxt/RUG01/002/479/620/RUG01-002479620_2018_0001_AC.pdf.
- [204] Till Neuhoffer. “Estimating the angular resolution of tracks in neutrino telescopes based on a likelihood analysis”. In: *Astropart. Phys.* 25 (2006), pages 220–225. DOI: 10.1016/j.astropartphys.2006.01.002. arXiv: astro-ph/0403367 [astro-ph].
- [205] URL: https://wiki.icecube.wisc.edu/index.php/SLC_hit_cleaning.
- [206] URL: <https://www.dissertations.se/dissertation/fef1f8e4ba/>.
- [207] Yoav Freund and Robert E Schapire. “A Decision-Theoretic Generalization of On-Line Learning and an Application to Boosting”. In: *Journal of Computer and System Sciences* 55.1 (1997), pages 119–139. ISSN: 0022-0000. DOI: <https://doi.org/10.1006/jcss.1997.1504>. URL: <http://www.sciencedirect.com/science/article/pii/S002200009791504X>.
- [208] S. Fink C. Böser and S. Röcker. *Introduction to boosted decision trees: A multivariate approach to classification problems*. Presented at the KSETA Doctoral Workshop, Berlin, Germany. July 2014.

-
- [209] Hanchuan Peng, Fuhui Long, and C. Ding. “Feature selection based on mutual information criteria of max-dependency, max-relevance, and min-redundancy”. In: *IEEE Transactions on Pattern Analysis and Machine Intelligence* 27.8 (Aug. 2005), pages 1226–1238. ISSN: 0162-8828. DOI: 10.1109/TPAMI.2005.159.
 - [210] The IceCube collaboration. URL: <https://docushare.icecube.wisc.edu/dsweb/Get/Document-56551/VEFproposal.pdf>.
 - [211] The IceCube collaboration. URL: https://docushare.icecube.wisc.edu/dsweb/Get/Document-59303/lowup_2012_proposal.pdf.
 - [212] The IceCube collaboration. URL: https://docushare.icecube.wisc.edu/dsweb/Get/Document-59906/MuonFilter2012_v3_with_addendum.pdf.
 - [213] The IceCube collaboration. URL: <https://docushare.icecube.wisc.edu/dsweb/Get/Document-59728/onlinel2proposal2012.pdf>.
 - [214] The IceCube collaboration. URL: <https://docushare.icecube.wisc.edu/dsweb/Get/Document-59397/DeepCoreFilterProposal.pdf>.
 - [215] IceCube collaboration. URL: https://wiki.icecube.wisc.edu/index.php/Effects_of_DOM_Mainboard_Release_443.
 - [216] S. Verpoest. “Search for particles with fractional charges in IceCube based on anomalous energy loss”. Master’s thesis. UGent, 2018.
 - [217] J. Künnen. “A Search for Dark Matter in the Center of the Earth with the IceCube Neutrino Detector”. Master’s thesis. VUB, 2015.
 - [218] R. J. Britto, B. S. Acharya, and G. C. Anupama. “Data analysis method for the search of point sources of gamma rays with the HAGAR telescope array”. In: *Proceedings, 32nd International Cosmic Ray Conference (ICRC 2011): Beijing, China, August 11-18, 2011*. Volume 9, page 142. DOI: 10.7529/ICRC2011/V09/0943.
 - [219] M. G. Aartsen et al. “Searches for Relativistic Magnetic Monopoles in IceCube”. In: *Eur. Phys. J.* C76.3 (2016), page 133. DOI: 10.1140/epjc/s10052-016-3953-8. arXiv: 1511.01350 [astro-ph.HE].
 - [220] F. Scheriau. “Data-Mining in der Astroteilchenphysik”. Master’s thesis. University of Dortmund, 2014.
 - [221] Gary J. Feldman and Robert D. Cousins. “A Unified approach to the classical statistical analysis of small signals”. In: *Phys. Rev.* D57 (1998), pages 3873–3889. DOI: 10.1103/PhysRevD.57.3873. arXiv: physics/9711021 [physics.data-an].
 - [222] Gary C. Hill and Katherine Rawlins. “Unbiased cut selection for optimal upper limits in neutrino detectors: The Model rejection potential technique”. In: *Astropart. Phys.* 19 (2003), pages 393–402. DOI: 10.1016/S0927-6505(02)00240-2. arXiv: astro-ph/0209350 [astro-ph].
 - [223] Aaron Roodman. “Blind analysis in particle physics”. In: *eConf* C030908 (2003). [,166(2003)], TUIT001. arXiv: physics/0312102 [physics.data-an].